Design, synthesis and biological activity of N^5-Substituted tetrahydropteroate analogs as non-classical antifolates against cobalamin-dependent methionine synthase and potential anticancer agents

Meng Wang, Chao Tian, Liangmin Xue, Hao Li, Jing Cong, Fang Fang, Jiajia Yang, Mengmeng Yuan, Ying Chen, Ying Guo, Xiaowei Wang, Junyi Liu, Zhili Zhang

PII: S0223-5234(20)30080-5

DOI: https://doi.org/10.1016/j.ejmech.2020.112113

Reference: EJMECH 112113

To appear in: *European Journal of Medicinal Chemistry*

Received Date: 18 December 2019

Revised Date: 28 January 2020

Accepted Date: 31 January 2020

Please cite this article as: M. Wang, C. Tian, L. Xue, H. Li, J. Cong, F. Fang, J. Yang, M. Yuan, Y. Chen, Y. Guo, X. Wang, J. Liu, Z. Zhang, Design, synthesis and biological activity of N^5-Substituted tetrahydropteroate analogs as non-classical antifolates against cobalamin-dependent methionine synthase and potential anticancer agents, *European Journal of Medicinal Chemistry* (2020), doi: https://doi.org/10.1016/j.ejmech.2020.112113.

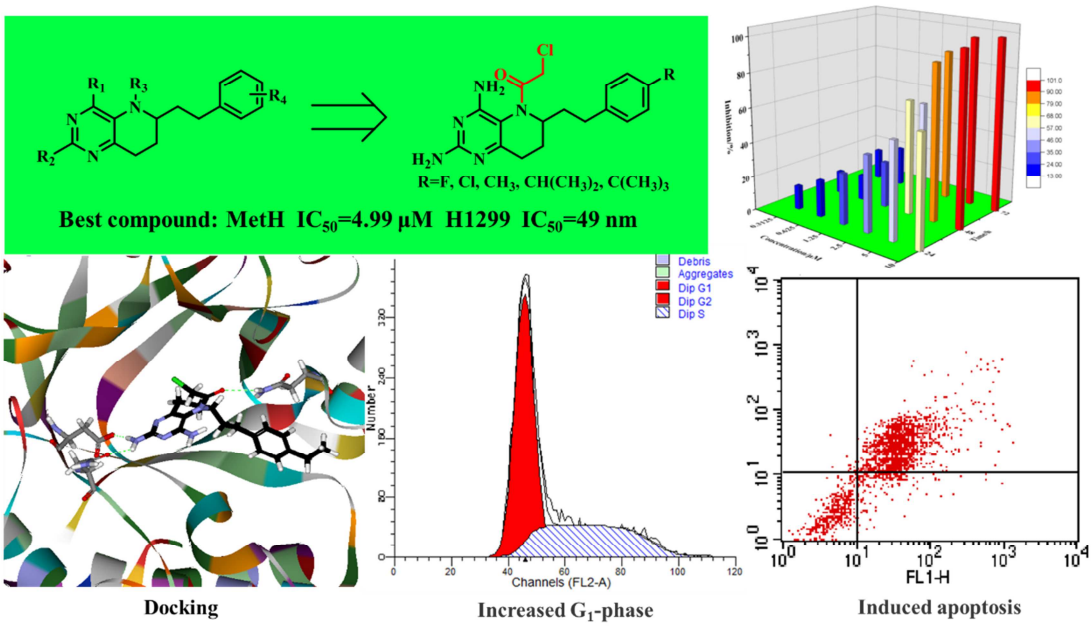

Docking

Increased G_1-phase

Induced apoptosis

Design, Synthesis and Biological Activity of N^5-Substituted Tetrahydropteroate Analogs as Non-classical Antifolates against Cobalamin-dependent Methionine Synthase and Potential Anticancer Agents

Meng Wang,[*,†,§] Chao Tian, [*,†] Liangmin Xue,[†] Hao Li,[†] Jing Cong, [†] Fang Fang,[†] Jiajia Yang,[†] Mengmeng Yuan,[†] Ying Chen,[†] Ying Guo,[†] Xiaowei Wang,[†] Junyi Liu,[†, ‡, ⊥] Zhili Zhang[†, ⊥]

[†]Department of Chemical Biology, School of Pharmaceutical Sciences, Peking University, Beijing 100191, China

[‡]State Key Laboratory of Natural and Biomimetic Drugs, Peking University, Beijing 100191, China

[§]College of Pharmacy, Beihua University, Jilin 132013, China

ABSTRACT: Cobalamin-dependent methionine synthase (MetH) is involved in the process of tumor cell growth and survival. In this study, a novel series of N^5-electrophilic substituted tetrahydropteroate analogues without glutamate residue were designed as non-classical antifolates and evaluated for their inhibitory activities against MetH. In addition, the cytotoxicity of target compounds was evaluated in human tumor cell lines. With N^5-chloracetyl as the optimum group, further structure research on the benzene substituent and on the 2,4-diamino group was also performed. Compound **6c**, with IC_{50} value of 12.1 μM against MetH and 0.16-6.12 μM against five cancer cells, acted as competitive inhibitor of MetH. Flow cytometry studies indicated that compound **6c** arrested HL-60 cells in the G_1-phase and then inducted late apoptosis. The molecular docking further explained the structure-activity relationship.

Keywords: pyrido[3,2-*d*]pyrimidine, methionine synthase, antifolate, inhibitor, anticancer

1. INTRODUCTION

Cobalamin-dependent methionine synthase (MetH), an important regulator of folate metabolism [1], catalyzes the transfer of methyl groups from the cofactor methyltetrahydrofolate (MTHF) to homocysteine (Hcy) to produce tetrahydrofolate (THF) and methionine (Met) [2].The cobalamin cofactor of MetH plays a crucial role in catalytic reaction which circulates between +1 and +3 oxidation states as methyl acceptor and methyl donor. During MetH reaction cycle the transfer of methyl group from MTHF to Met is in two steps by two nucleophilic substitution reactions. Firstly, the methyl group is transferred from MTHF to cofactor cob(I)alamin (Cbl(I)) to generate methylcob(III)alamin. Secondly, the methylcob(III)alamin is demethylated by Hcy to form cob(I)alamin again (**Figure 1**) [3-5].

[⊥]Corresponding author. Tel.: +86 10 82805203.
E-mail address: lilybmu@bjmu.edu.cn (J. Liu).
Chao Tian (co-first author)

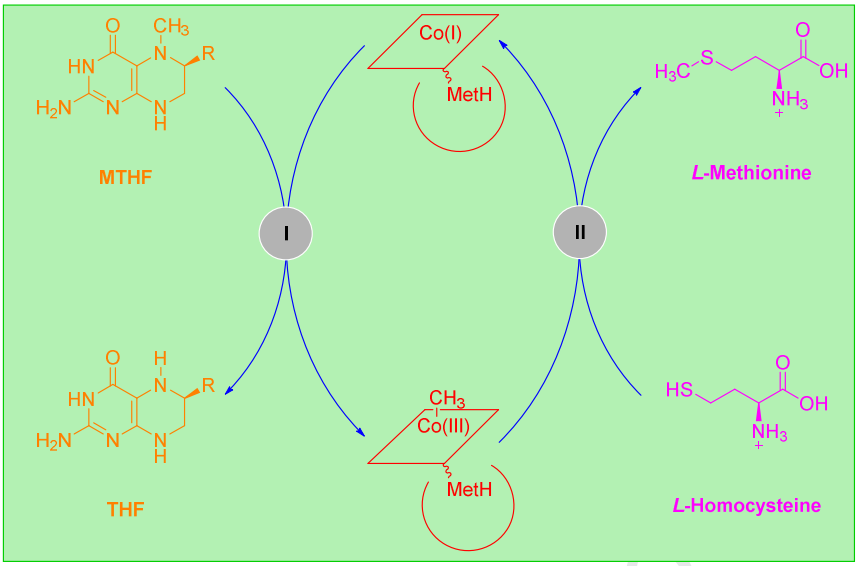

Figure 1. The cobalamin-dependent methionine synthase reaction.

Both cobalamin-dependent and cobalamin-independent forms of methionine synthase could be found in microorganisms, while the former in mammalian tissues and the latter in higher plant [6-8]. In humans, the primary circulating folate is MTHF, with sufficient physiological concentrations of ~5-30 nM in the blood [9]. It is well known that MetH is the only human enzyme that metabolizes MTHF to regenerate the active form THF. Therefore, it is essential in many important biochemical pathways, including folate cycles and one-carbon methionine transmethylation [10, 11]. In folate cycles, THF is transformed to other bioactive folates that provide one-carbon units for purine and pyrimidine synthesis [12, 13]. Met, a nutritionally essential amino acid and component of proteins, can be transformed to the active s-adenosyl methionine (SAM) which is an important methyl donor involved in biologically methylations of DNA, RNA, proteins, lipids and polyamine [14, 15]. Thus, impaired function of MetH could provide a valuable target for chemotherapeutic intervention in cancer [16].

Although it is recognized that MetH is an excellent target for rational drug design, there are a few studies on MetH inhibitors for anticancer. It was reported that some non-drug like inhibitors, including nitrous oxide (N_2O) [17], nitric oxide (NO) [18, 19], sodium nitroprusside [20] and ethanol [21], inhibited the enzyme through oxidation of the cobalamin cofactor. Methylmercury [22] and cobalamin analogs [23-25] were reported as non-drug like inhibitors too. However, there is less study on drug-like MetH inhibitors.

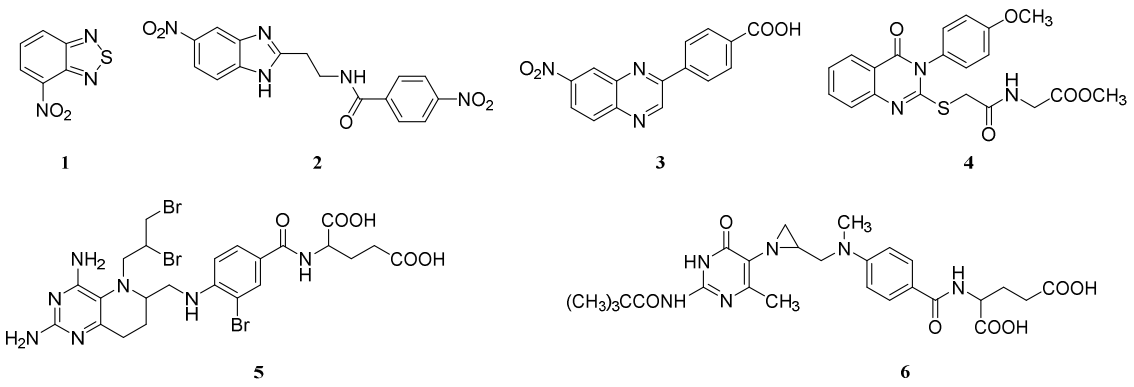

Figure 2. Structures of recently published MetH inhibitors.

Recently, novel benzothiadiazole (**1**), benzimidazole (**2**), quinoxaline (**3**) and analogues of quinazoline derivatives (**4**) were designed to mimic the substructure of MTHF, and evaluated for their activities against purified rat liver MetH (**Figure 2**) [26-28]. N^5-substituted 8-deazatetrahydrofolates (**5**) and aziridine tetrahydrofolate analogs (**6**) were designed and synthesized in our previous work, which could bind to MetH in place of MTHF by the formation of covalent bonds with the nucleophilic Cbl(I) cofactor and then inhibit methyl transfer [29, 30]. Though exhibiting certain inhibitory activities against MetH of HL-60 cells, these compounds share the shortcomings of classical antifolates because of their folate-like structures including the glutamic acid side chain. Classical antifolates, such as methotrexate (MTX), raltitrexed (RTX), pemetrexed (PMX) and pralatrexate (**Figure 3**) can't passively diffuse across cell membranes and must be actively transported using folate receptors (FRα, FRβ, FRγ), reduced folate carrier (RFC), or the proton-coupled folate transporters (PCFT) [31-34]. And, N^5-substituted 8-deazatetrahydrofolates and aziridine tetrahydrofolate analogs [29, 30] undergo the same intracellular metabolic processing, where folylpolyglutamate synthase (FPGS)-mediated polyglutamylation is a crucial determinant of their intracellular retention and pharmacological activity [35]. The impairment of the destroyed transport and polyglutamation mechanisms through genetic mutation can cause the resistance, which is the obvious shortcoming of classical anfitolates [36].

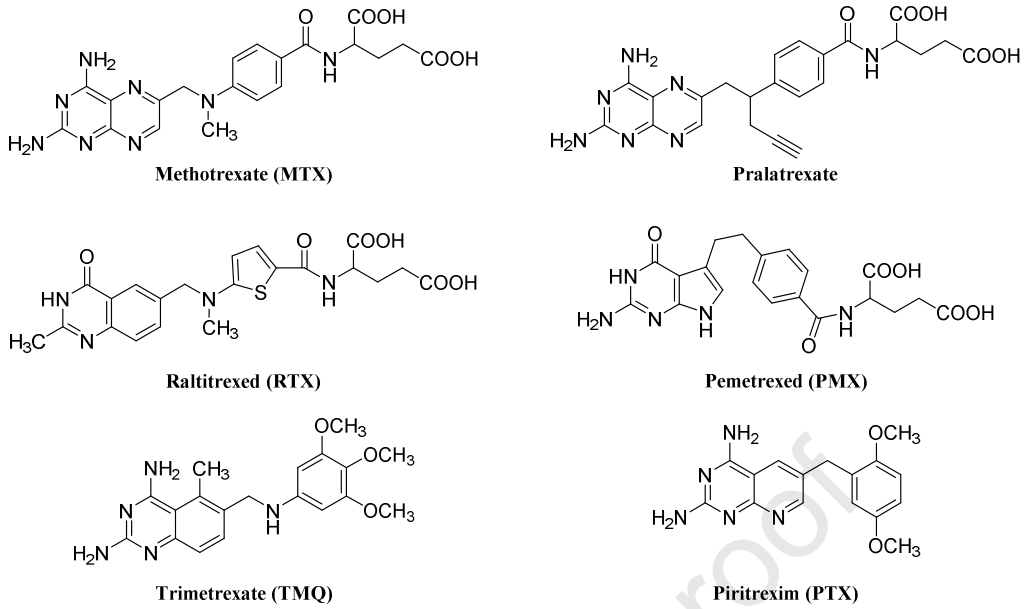

Figure 3. Structures of classical and nonclassical antifolates.

In contrast, nonclassical antifolates without glutamic acid moiety can penetrate cells through passive diffusion and act with no need of polyglutamylation, thus can overcome resistance of classical antifolates. Lipophilic nonclassical antifolates [37, 38], such as piritrexim and trimetrexate **(Figure 3)**, have demonstrated significant growth inhibition of tumor cell. There has been a continuing effort in our laboratory to develop novel nonclassical MetH inhibitor based on N^5-position substituted 8-deazatetrahydrofolates. The aim of the present study was to design and synthesize more lipophilic derivatives that lack a glutamate tail and to explore structure-activity relationships within a series of N^5-position substituted tetrahydropyrido[3,2-*d*]pyrimidines and different substituents of benzene ring (**Figure 4**).

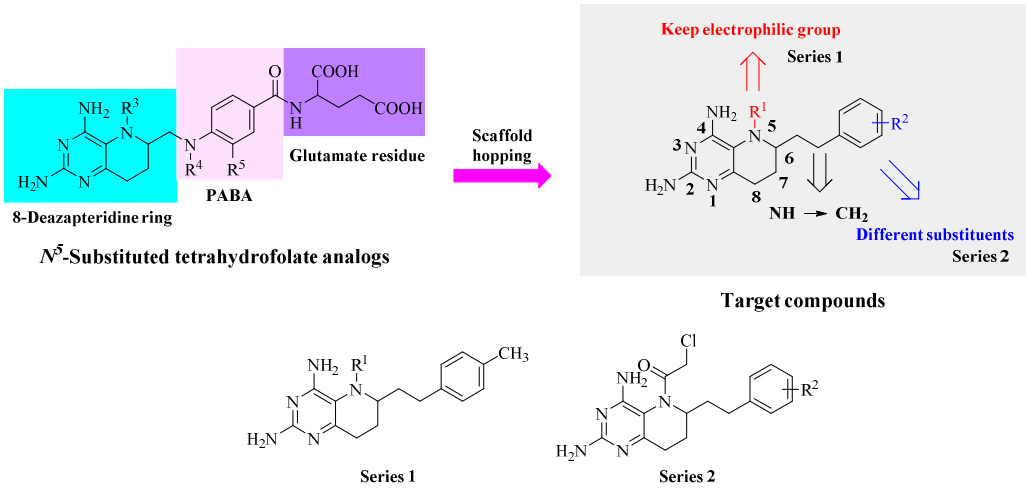

Figure 4. Design of novel N^5-substituted tetrahydropyrido[3,2-*d*]pyrimidines.

2. RESULTS AND DISCUSSION

2.1 Design and synthesis of N^5-substituted compounds in series 1.

Among the N^5-substituted tetrahydropteroate analogues, compounds with dibromopropyl and formyl groups on N^5 position showed the greatest activities against MetH with IC_{50} of 1.43-8.11 μM (**Figure 4**) [29]. So, more electrophilic groups, such as formyl, acryloyl, isopropanecarbonyl, chloroacetyl, chloroethyl, 3-chloropropionyl, 3-chloropropyl and bromoacetyl groups, were designed on N^5-position to research the influence of electrophilicity, size and steric hindrance of substituents besides truncation of the glutamate tail present in classical antifolates. Considering the potential flexibility and better lipid solubility, a C−C bridge between pyridopyrimidine and aryl ring is necessary compared with C-N bridge [39-42], thus leading to our first design of the compound series 1 (**Figure 4**).

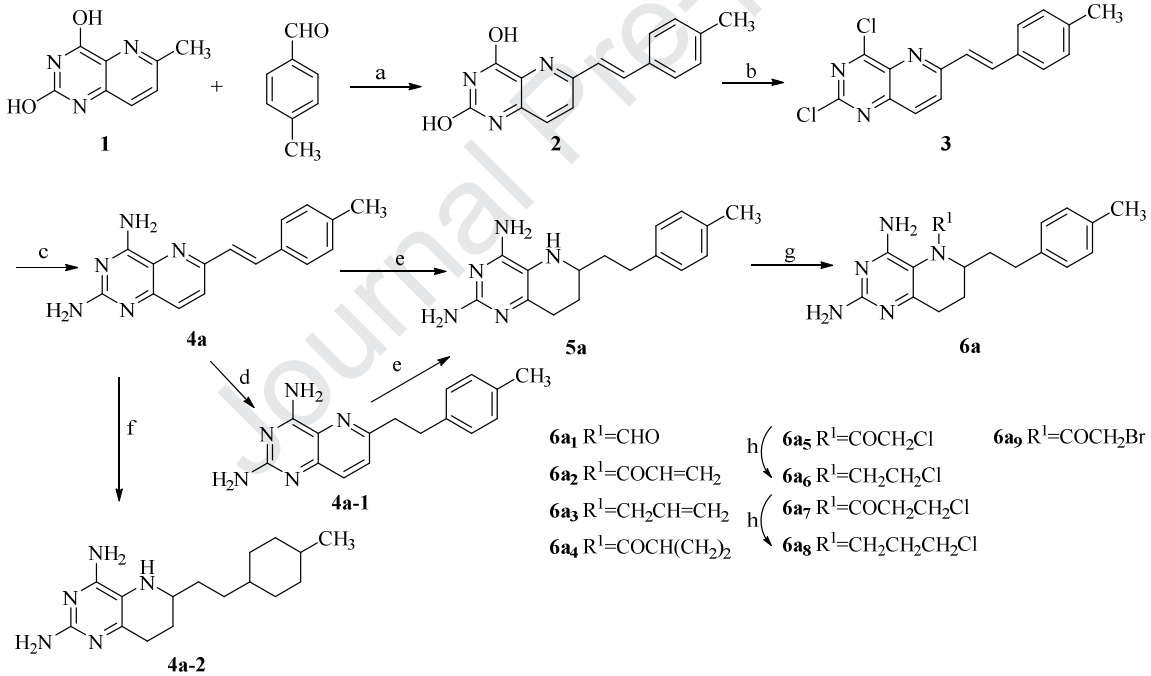

Scheme 1. Reagents and conditions: (a) *p*-toluenesulfonamide, *N*,*N*-dimethylacetamide, 160 ^{o}C, 36 h; (b) $POCl_3$, Et_3N, reflux, 8 h; (c) saturated NH_3 in dry methanol, 150 ^{o}C, 8 h; (d) Pd/C, ethanol, rt, 12 h; (e) PtO_2 , ethanol, 0.5 mol/L HCl, rt, 12 h; (f) PtO_2 , ethanol, 2 mol/L HCl, rt, 12 h; (g) **$6a_1$**: HCOOH, $(CH_3CO)_2O$, CH_2Cl_2; **$6a_2$**, **$6a_3$**, **$6a_4$**, **$6a_5$**, **$6a_7$**, **$6a_9$**,: acryloyl chloride, allyl bromide, isopropanecarbonyl chloride, chloroacetyl chloride, 3-chloropropionyl chloride, bromoacetyl chloride, respectively, anhydrous DMF, rt; (h) BH_3-THF, THF, rt.

Target compounds **$6a_1$**-**$6a_9$** were prepared via the synthetic route outlined in **Scheme 1**. Using the Skraup reaction previously described, 5-aminouracil and croton aldehyde were cyclized in 20% HCl to give 2,4-dihydroxy-6-methylpyrido[3,2-*d*]pyrimidine (**1**) in good yield [43]. Then alkenylation of compound **1**

with *p*-methyl benzaldehyde and *p*-toluenesulfonamide via sp^3 C-H bond activation in DMAC achieved (*E*)-6-(4-methylstyryl)pyrido[3,2-*d*]pyrimidine-2,4(1H,3H)-dione (**2**) in one-step in 91% yield [44]. Treatment of compound **2** with a large excess of $POCl_3$ produced 2,4-dichloride derivative (**3**) in 65% yield. Then compound **3** was reacted directly with a saturated solution of ammonia in methanol in a sealed vessel at 150 °C for 8 h to give a light yellow solid (**4a**) in 95% yield [45]. Hydrogenation of the carbon-carbon double bonds and pyridine ring in compounds **4a** with PtO_2 and 0.5 mol/L HCl in ethanol at room temperature gave compound **5a** in excellent yields. When 2 mol/L HCl was used in reaction, cyclohexyl product **4a-2** was produced. But when Pd/C was used as catalyst, only the double bond was reduced to give **4a-1**. With the reduction product **5a** in hand, treatment with a mixture of acetic anhydride and formic acid gave the N^5-formyl derivative $\mathbf{6a_1}$ directly. The N^5-chloracetyl and bromoacetyl derivatives $\mathbf{6a_5}$, $\mathbf{6a_9}$ were obtained in good yields by chloroacetylation and bromoacetylation of **5a**. Similarly, compound **5a** was acylated by 3-chloropropionyl chloride to give N^5-3-chloropropionyl derivative $\mathbf{6a_7}$. The N^5-chlorinated acyl derivatives $\mathbf{6a_5}$ and $\mathbf{6a_7}$ were then converted to N^5-2-chloroethyl derivative $\mathbf{6a_6}$ and 3-chloropropyl derivative $\mathbf{6a_8}$ by BH_3-THF in THF. Other N^5-acyl and allyl derivatives $\mathbf{6a_2}$-$\mathbf{6a_4}$ were obtained by acylation and allylation of **5a** in good yields.

2.2 Preliminary Evaluation of Compounds 6a$_1$-6a$_9$.

Table 1 Chemical structures and in vitro inhibitory activities against tumor cells and MetH of the N^5-position substituted pyrido[3,2-*d*]pyrimidines in series 1.

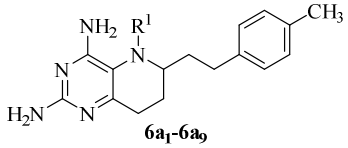

$\mathbf{6a_1}$-$\mathbf{6a_9}$

Compounds	R^1	Tumor cells (IC_{50}, μM)[b]					MetH (IC_{50}, μM)[b]
		H1299	A549	HL-60	HeLa	HT29	
$\mathbf{6a_1}$	CHO	>100	74.6±1.1	24.7±0.6	>100	>100	10.8%[c]
$\mathbf{6a_2}$	$COCH=CH_2$	18.5±1.3	59.9±1.8	9.93±0.24	27.1±4.1	46.3±0.8	13.4%[c]
$\mathbf{6a_3}$	$CH_2CH=CH_2$	9.75±0.37	9.52±0.31	1.65±0.24	12.9±0.1	26.2±0.6	41.6%[c]
$\mathbf{6a_4}$		>100	>100	12.2±1.1	65.8±4.4	72.5±2.7	22.0%[c]
$\mathbf{6a_5}$	$COCH_2Cl$	0.21±0.02	1.97±0.03	0.39±0.06	1.46±0.07	4.74±0.43	5.66±0.49
$\mathbf{6a_6}$	CH_2CH_2Cl	17.7±1.6	18.1±0.6	2.38±0.05	21.4±0.9	20.7±0.6	37.5%[c]

6a$_7$	$COCH_2CH_2Cl$	85.3±5.5	>100	21.8±1.5	69.5±6.3	>100	46.9%[c]
6a$_8$	$CH_2CH_2CH_2Cl$	15.9±2.8	25.1±2.6	1.04±0.10	22.8±1.2	20.7±1.8	30.0%[c]
6a$_9$	$COCH_2Br$	0.99±0.19	ND[a]	1.60±0.16	ND[a]	6.14±0.84	48.0±2.9
MTX	/	0.072±0.001	0.014±0.002	0.023±0.001	>100	>100	ND[a]

[a] Not tested. [b] Indicates the average value of three independent experiments. [c] Inhibition% at 100 μM.

The N^5-electrophilic substituted compounds then were tested for their antiproliferative activities against MetH and five human tumor cell lines. Besides HL-60 (human promyelocytic leukemia), A549 (human lung) and H1299 (human lung) based on the clinical effect of antifolates MTX and Pemetrexed, HeLa (cervix) and HT29 (colon cancer) were also chosen because of their relative high incidence [46] (**Table 1**). Among the five cell lines, HL-60 cell lines were most sensitive to the cytotoxic effects of target compounds with the IC_{50}s of 0.39-25 μM. While big difference of H1299, A549, HeLa and HT29 cell inhibition between **6a$_1$**-**6a$_9$** was observed. **6a$_5$** and **6a$_9$**, with the N^5-chloracetyl and bromoacetyl group respectively, exhibited the notable activities against the tumor cells as IC_{50}s of 0.2-4.7 μM and 1.0-6.1 μM. The result is consistent with what had been observed in the inhibition against MetH, in which IC_{50} values of **6a$_5$** and **6a$_9$** (IC_{50} values 5.66 μM and 48.0 μM respectively) were more potent than others (IC_{50} values >100 μM).

It was apparent that the chloracetyl and bromoacetyl groups at N^5-position were associated with stronger inhibition against MetH than other subtitutents. They showed excellent activities compared to the MetH inhibitors reported in literatures such as benzothiadiazoles with IC_{50} >95 μM [26], benzimidazole with IC_{50} >50 μM besides two derivatives with IC_{50} value of about 18 μM ,quinoxalines with IC_{50} >70 μM besides only one derivative with IC_{50} value of 9 μM and quinazolines with inhibition of 60% at 100 μM [27, 28].The significant difference of biochemical activities between **6a$_5$** (N^5-chloroacetyl group, 5.66 μM), and **6a$_6$** (***N***^{5}-chloroethyl group, >100 μM**)** and **6a$_7$** (N^5-chloropropionyl group, >100 μM) illustrated the necessity of the carbonyl and *β*-chloride groups in N^5 substituent. Compound **6a$_5$** with 5-chloracetyl group were approximately 10-fold more potent than 5-bromoacetyl compound **6a$_9$**. The corresponding N^5-chloroethyl compound **6a$_6$** was less potent than N^5-chloracetyl compound **6a$_5$** whether against tumor cells (9.0-87.3 μM verse 0.2-4.7 μM) or MetH (>100 μM verse 5.66 μM).

The results of compounds **6a$_1$**, **6a$_5$**, **6a$_6$**, **6a$_7$** and **6a$_9$** indicated that both carbonyl and halogen atom at its *β*-position on N^5-position were necessary for activities against MetH. The function of carbonyl group will be studied further in the molecular modeling section to understand the binding activity to active site of

MetH.

2.3 Structure-Activity Relation Research Based on Lead Compound 6a$_5$.

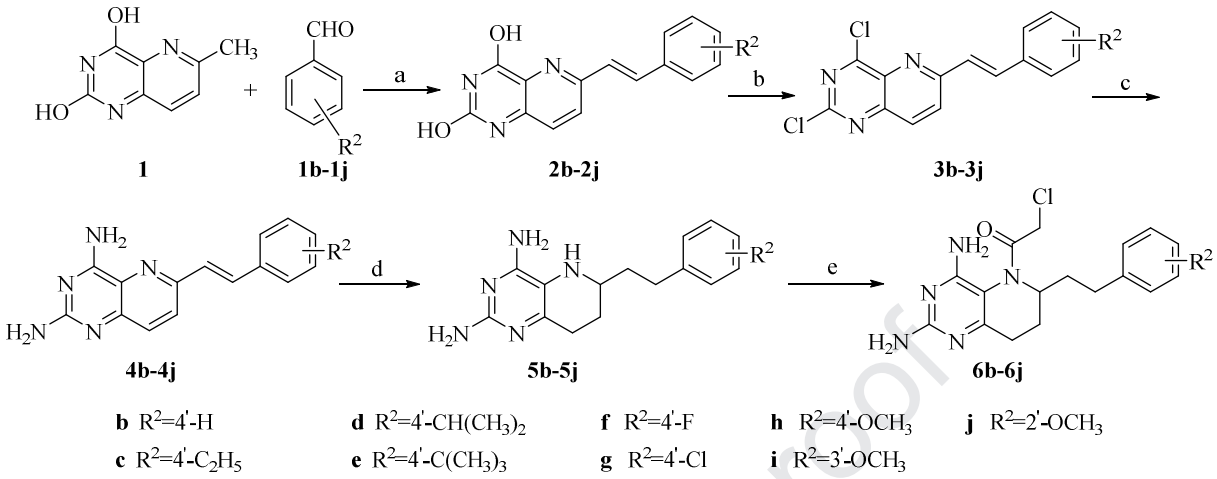

Scheme 2. Reagents and conditions: (a) *p*-toluenesulfonamide, *N*,*N*-dimethylacetamide, 160 ^{o}C, 36 h; (b) $POCl_3$, Et_3N, reflux, 8 h; (c) saturated NH_3 in dry methanol, 150 ^{o}C, 8 h; (d) PtO_2, 0.5 mol/L HCl, ethanol, rt; (e) acetyl chloride, anhydrous DMF, rt.

In view of the structural novelty with N^5- electrophilic groups, we selected compound **6a$_5$** as lead inhibitor for further structural optimization. To identify the structure activity relationships of substituents on benzene, electron-donating groups (ethyl, isopropyl and t-butyl) were chosen as the *p*-substitution based on the methyl group of **6a$_5$**. Methoxyl group was also selectived as electron-donation substitutent, and attached at different positions on the benzene ring as *o*-, *m*- and *p*-position. Beyond that, halogen electron-withdrawing groups such as fluorine and chloride were attached at *p*-position of benzene ring too. Compounds **6b-6j** of series 2 were designed and successfully synthesized (**Scheme 2)**. The target compounds were tested for their inhibitory activity against MetH of HL-60, and the half-inhibitory concentrations (IC_{50}s) are presented in **Table 2**.

Table 2 Chemical structures and in vitro inhibitory activities against tumor cells and MetH of the N^5-chloroacetyl pyrido[3,2-*d*]pyrimidines in series 2

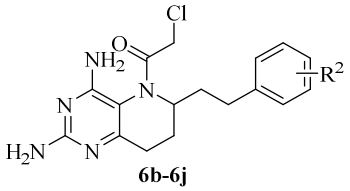

Compounds	R^2	Tumor cells (IC_{50}, μM)[a]					MetH (IC_{50}, μM)[a]
		H1299	A549	HL-60	HeLa	HT29	
6b	H	0.44±0.06	4.42±0.45	0.63±0.05	1.82±0.60	3.43±0.54	45.8%[b]

6c	4'-C_2H_5	0.16±0.01	6.12±0.38	0.53±0.01	0.85±0.16	3.02±0.18	12.1±1.0
6d	4'-$CH(CH_3)_2$	0.093±0.018	3.13±0.30	0.32±0.01	2.16±0.79	3.43±0.54	45.9±3.6
6e	4'-$C(CH_3)_3$	0.049±0.007	3.13±0.30	0.20±0.01	0.44±0.16	1.14±0.03	13.5±1.8
6f	4'-F	0.23±0.05	1.16±0.04	0.79±0.03	0.96±0.20	2.96±0.27	4.99±0.85
6g	4'-Cl	0.12±0.02	4.35±0.40	0.46±0.01	1.52±0.51	3.49±0.02	14.9±0.78
6h	4'-OCH_3	0.57±0.16	6.16±0.33	0.63±0.05	2.71±0.12	5.62±0.69	46.1%[b]
6i	3'-OCH_3	0.24±0.07	1.51±0.13	0.34±0.01	1.64±0.06	5.55±0.52	42.6%[b]
6j	2'-OCH_3	0.66±0.02	2.31±0.06	0.95±0.05	5.25±0.78	4.83±0.06	51.5±4.5

[a] Indicates the average value of three independent experiments. [b] Inhibition% at 100 μM.

Compared with the analogues of series 1 (IC_{50}=0.21- >100 μM) in **Table 1**, **6b-6j**, with N^5-chloracetyl substituent, exhibited more potent inhibitory activities against all five tumor cells (IC_{50}=0.049-6.16 μM). Besides **6b**, **6h** and **6i**, all N^5-chloracetyl compounds (**Table 2**) showed better activities against MetH compared with the analogues except **$6a_5$** and **$6a_9$** in **Table 1**. Among them, **6d** and **6j** exhibited activities with IC_{50} of about 51 μM, and **6c**, **6e**, **6f**, **6g** with IC_{50s} below 20 μM. The results indicated that the N^5-chloroacetyl group in series 2 could increase the inhibition against both tumor cells and MetH.

Contrasted to **6b** without substituent on benzene ring, alkyl substituted compounds **$6a_5$**, **6c**, **6d** and **6e** showed more potent activities. They inhibited MetH activities in the following order of potency (substituents on benzene moiety are noted in parentheses): **$6a_5$** (5.66 μM, methyl group) > **6c** (12.1 μM, ethyl group) > **6e** (13.5 μM, *tert*-butyl group) > **6d** (46.9 μM, isopropyl group). **6f** and **6g** with halogens substituted on the *p*-position of benzene maintained the potent inhibition as IC_{50} values 4.99 μM and 14.9 μM. But the methoxyl group, whether in *o*-, *m*-position or *p*-position (**6j**, **6i**, **6h**), didn't cause any significant increase of potency (IC_{50} values as >100 μM, >100 μM and 51.5 μM).

Though with chloracetyl group on N^5 position, compounds **6b**, **6h** and **6i** didn't show MetH inhibition. Their normal inhibitory activity against the five tumor cells revealed that they might act on folic acid metabolizing enzyme such as DHFR or thymidylate synthetase based their folate-like structure of substrate [47]. Or their N^5-chloroacetamido group might afford certain effect similar with biological alkylating agent [48].

2.4 Synthesis and in vitro Inhibitory Activities of Series 3.

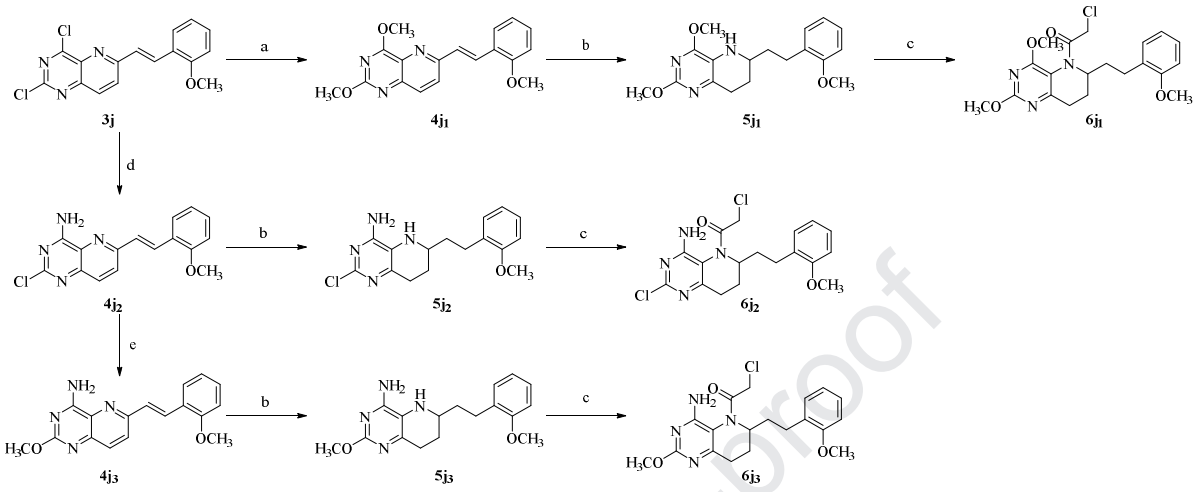

Scheme 3. Reagents and conditions: (a) CH_3ONa, CH_3OH, reflux, 8 h; (b) 0.4 MPa H_2, PtO_2, 0.5 mol/L HCl, ethanol, rt; (c) acetyl chloride, anhydrous DMF, rt; (d) saturated NH_3 in dry methanol, rt, 12 h; (e) CH_3ONa, CH_3OH, reflux, 5 h.

The study of structure-activity relationship revealed the importance of N^5-chloracetyl and the substitution of benzene in target compounds for the activities against MetH. To test the indispensability of the amino groups at 2 and 4 position for the inhibition of MetH activities, amino group was replaced by chloride or methoxyl group as in series 3. The synthetic route was outlined in **Scheme 3**. With compound **3j** in hand as in series 2, methoxylation of 2,4-chloride group with sodium methoxide in methanol gave dimethoxylated compound **$4j_1$** in 72% yield. Selectively amination on 4-chloride group of compound **3j** gave **$4j_2$** in good yield which was then methoxylated on the 2-chloride to afford **$4j_3$** in 70% yield. Compounds **$5j_1$**, **$5j_2$** and **$5j_3$** were then prepared by hydrogenation of the carbon-carbon double bonds and pyridine ring of **$4j_1$**, **$4j_2$** and **$4j_3$** with H_2 and PtO_2 in excellent yield, followed by N^5-chloroacetylation to get **$6j_1$**, **$6j_2$** and **$6j_3$**.

The IC_{50}s of **$6j_1$**, **$6j_2$** and **$6j_3$** against MetH were all above 100 μM, which proved that 2,4-diamino of N^5-chloracetyl derivatives was the necessary group for inhibition of MetH. The further research was in the molecular modeling section. It is noticed that compounds **$6j_1$-$6j_3$** exhibited good inhibition effect against H1299, A549, HL-60, HeLa and HT29 tumor cells. So the action of N^5-chloroacetyl group in **$6j_1$**, **$6j_2$** and **$6j_3$** as possible alkylation agent or on folate metabolic enzymes besides MetH will be explored in the future [47, 48].

Table 3 Chemical structures of **6j$_1$-6j$_3$** and in vitro inhibitory activities against tumor cells and MetH

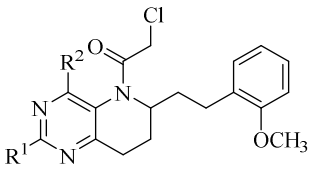

6j$_1$-6j$_3$

Compounds	R^1	R^2	Tumor cells (IC_{50}, μM)[b]					MetH[c]
			H1299	A549	HL-60	HeLa	HT29	
6j$_1$	OCH_3	OCH_3	0.47±0.03	>10	3.41±0.16	6.80±0.50	4.54±0.30	5.69%
6j$_2$	Cl	NH_2	0.32±0.07	3.35±0.41	0.24±0.02	0.94±0.19	2.52±0.21	45.6%
6j$_3$	OCH_3	NH_2	0.41±0.08	ND[a]	0.51±0.02	1.83±0.48	4.82±0.70	31.5%

[a] Not tested. [b] Indicates the average value of three independent experiments. [c] Inhibition% at 100 μM.

2.5 Action Mechanism of the MetH Inhibition.

We next studied the preliminary mechanism of action of the MetH inhibition by compound **6c** via three different concentrations of the substrate MTHF at a fixed concentration of Hcy (500 μM) and cell lysates. As illustrated in **Figure 5**, inhibition of MetH by **6c** decreased with increasing concentrations of MTHF. When addition of MTHF at 63 μM, IC_{50} value of **6c** was 4.46 μM. And when addition with higher concentration of MTHF at 126 and 252 μM, lower inhibition of **6c** was detected with IC_{50} values as 7.64 and 12.1 μM, respectively. At high substrate concentrations the action of **6c** was overcome which indicated that compound **6c** was a competitive inhibitor to MetH.

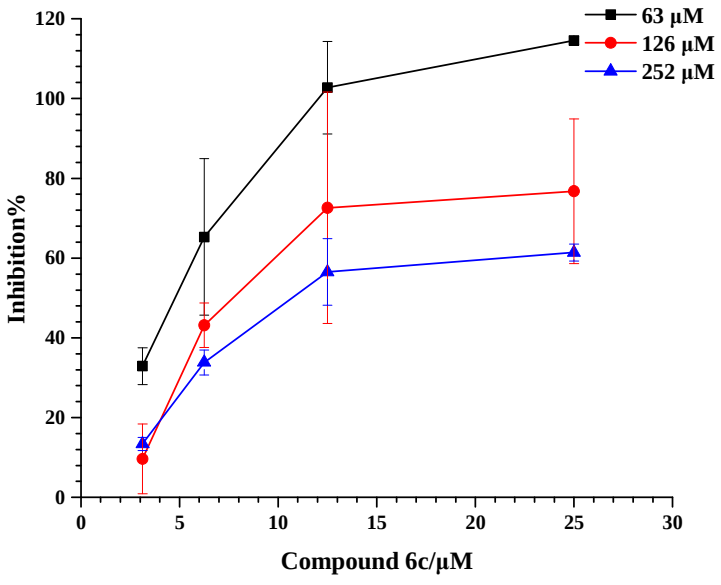

Figure 5. Effect of compound **6c** on MetH activity of HL-60 at MTHF concentrations of 63, 126 and 252 μM.

2.6 Dose-response Curves of 6c and 6a$_5$.

Cell proliferation inhibition of compounds **6c** and **6a$_5$** was measured over 0.3125, 0.625, 1.25, 2.5, 5 and 10 μM in 24 h, 48 h and 72 h. When at 0.3125 and 0.625 μM, **6c** caused growth inhibition of cancer cells below 50% even after 72 h. When **6c** was 1.25 μM, the inhibition was below 50% after 48 h, and about 95% after 72 h. When **6c** was 2.5 μM and above, the inhibition was about 95% even after 48 h. Compound **6a$_5$** of 1.25 μM exhibited the inhibition below 50% after 48 h and about 65% after 72 h. Compound **6a$_5$** of 1. 25, 2.5, 5 and 10 μM did not show the activities as good as **6c**, but the effect of concentration and time were consistent with what had been observed in compound **6c**. They exhibited a dose-response curve and a time-response curve.

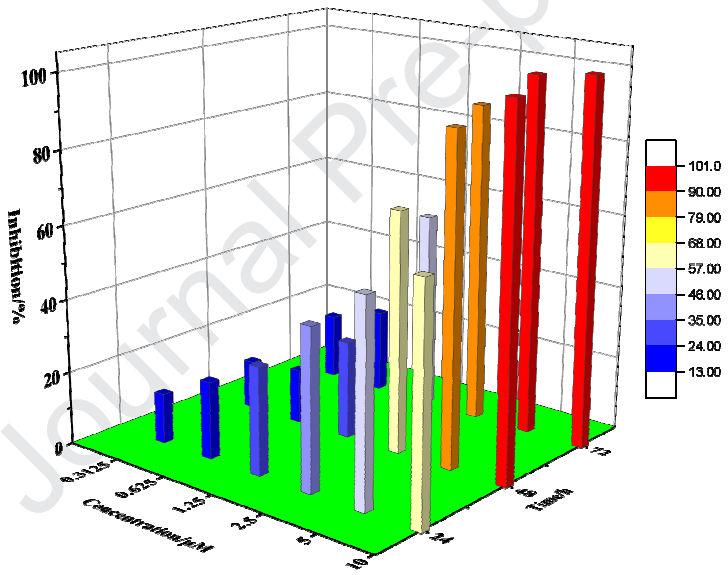

Figure 6 Dose-dependent effects of **6c** were incubated for 24, 48 and 72 h. A549 cell viabilities (densities) were determined by MTS assay. Each data point represents the average value from three independent experiments.

2.7 Cell cycle assay of 6c on HL-60 cells.

The effects of **6c** on the cell-cycle progression in HL-60 cells were investigated as well. After 24 h treatment with HL-60 cells, 0.5 μM and 0.75 μM of **6c** was found to significantly arrest cell cycle progression at G_1 cells in a dose-dependent manner (36.99 and 61.97 versus 32.08% in control) (**Figure 7**) . And a decrease in the amount of G_2/M cells (5.69, and 0.34 versus 11.21% in control) was observed too. The results suggested that compound **6c** induced a G_1 cell cycle block, which could slow down the

proliferation of HL-60 cells. The data of the cell cycle assay indicated that compound **6c** inhibited HL-60 proliferation in the same way as the classic inhibitors of MetH [29, 49].

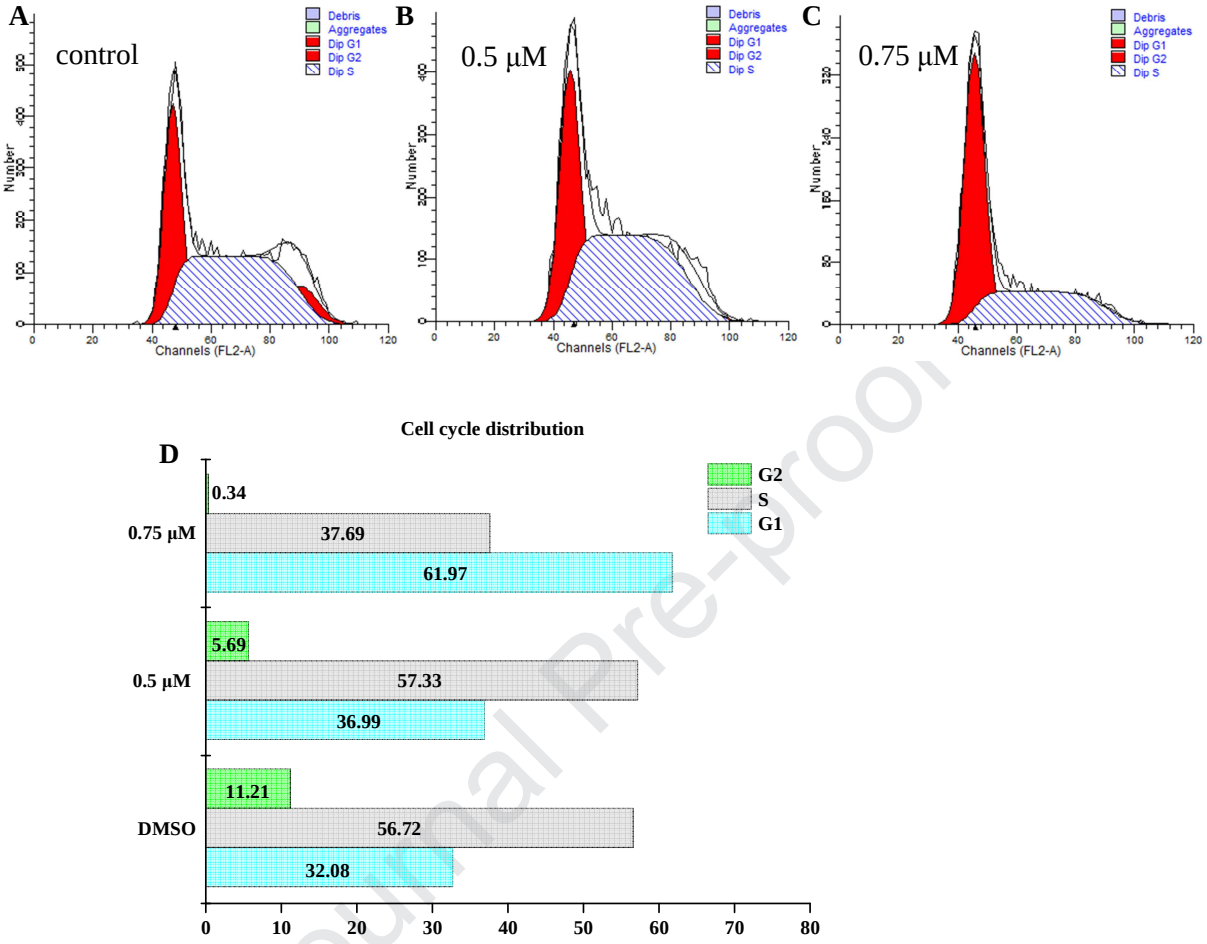

	DMSO	0.5 μM	0.75 μM
G_1	32.08%	36.99%	61.97%
S	56.72%	57.33%	37.69%
G_2	11.21%	5.69%	0.34%

Figure 7. Cell cycle assay. Cell cycle distribution was detected by flow cytometry. **A**) DMSO; **B**) Compound **6c** (0.5 μM); **C**) Compound **6c** (0.75 μM); **D**) The percentage of cells in different phase of cell cycle.

2.8 Apoptosis analysis.

HL-60 cells were treated with compound **6c** (0.5 μM and 0.75 μM) for 48 h to assess its effect on induction of apoptosis. The fraction of cells in late apoptosis was 2.35%, 2.18%, and 70.04% for control cells, cells treated with compound **6c** (0.5 μM), and cells treated with compound **6c** (0.75 μM), respectively (**Figure 8**). The corresponding fractions of cells in early apoptosis were 2.32%, 3.97%, and 8.71%. These results indicated that higher concentrations of compound **6c** induced more apoptosis, especially in the in

late apoptosis which was 30-fold after being exposed to 0.75 μM of **6c.** The data suggested that **6c** blocked HL-60 cells at of G_1 phase and then induced the late apoptosis which was about the anti-proliferative effect.

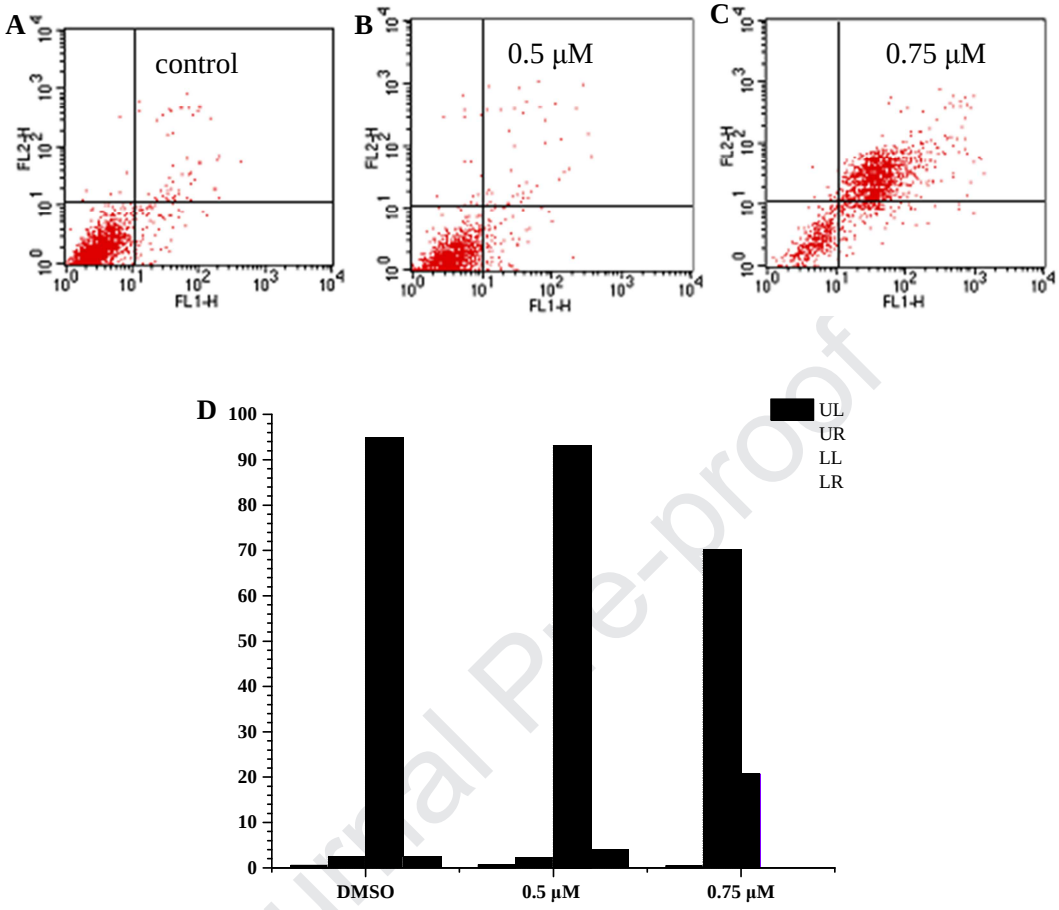

Compound	Concentration (μM)	UL	UR	LL	LR
DMSO		0.53	2.35	94.81	2.32
6c	0.5	0.67	2.18	93.17	3.97
6c	0.75	0.49	70.04	20.76	8.71

Figure 8. Analysis of apoptosis by Annexin V-FITC/PI staining and flow cytometry is shown for HL-60 cells treated with compound **6c** along with untreated control. **A**) DMSO; **B**) Compound **6c** (0.5 μM); **C**) Compound **6c** (0.75 μM); **D**) UL: dead cells; UR: late apoptosis cells; LL: viable cells; LR: early apoptosis cells.

2.9 Molecular Modeling.

In order to investigate the binding mode of the inhibitors to MetH, compound **6c** was selected for molecular docking experiments as it showed good in vitro inhibitory activity against MetH and tumor cells. It was performed using MTHF-binding pocket of a homology model of the human MetH with the ligand

minimization of Discovery Studio 2.5. As shown in **Figure 9. A**, compound **6c** (black) bound to MetH in the same pocket and in same extended mode as MTHF (blue), except the difference of molecular length. This results was consistent with our biological assay of compound **6c,** which acted as MetH competitive inhibitor. Besides the hydrogen bonds formed by 2-NH_2 with residues Asp 525 and Asn 527, the N^5-carbonyl oxygen could afford another one with residue Asn 367. This modeling result revealed that the N^5-chloracetyl on the N^5-position was conducive to binding position and binding mode too, which was important for the potency of MetH inhibition.

Compounds **6c**, **6j** and **6a$_5$**, all with N^5-chloracetyl group, differ only in the substituent of benzene (*p*-methyl in **6c**, *o*-methoxyl group in **6j** and *p*-ehthyl group in **6a$_5$**). **6c** (black, **Figure 9. B**) and **6a$_5$** (yellow, **Figure 9. D**) were able to establish same hydrogen bonds with the side chain of Asp-525, Asn-527 and Asn-367. Unlike the binding mode of compounds **6c** and **6a$_5$**, backbone of **6j** (deep red, **Figure 9. C**) rotated and formed hydrogen bonds in different orientation because of the *o*-methoxyl group, which was consistent with the reduced activity. More details were provided in the Supplementary Material (**Figure 10**). Compared with **6c** and **6j** respectively, **6a$_6$** (green, **Figure 9. E**) with chloroethyl on the N^5-position and **6j$_2$** (red, **Figure 9. F**) with chloride substitution in 2-position could establish only one hydrogen bond interaction each with backbone residue. Accordingly IC_{50s} of **6a$_6$** and **6j$_2$** against MetH were over 100 μM. The observation could explain the reason for higher inhibition on MetH of **6c** and the significant activity difference between compounds with various substituents on N^5-position, 2,4-position and benzene ring.

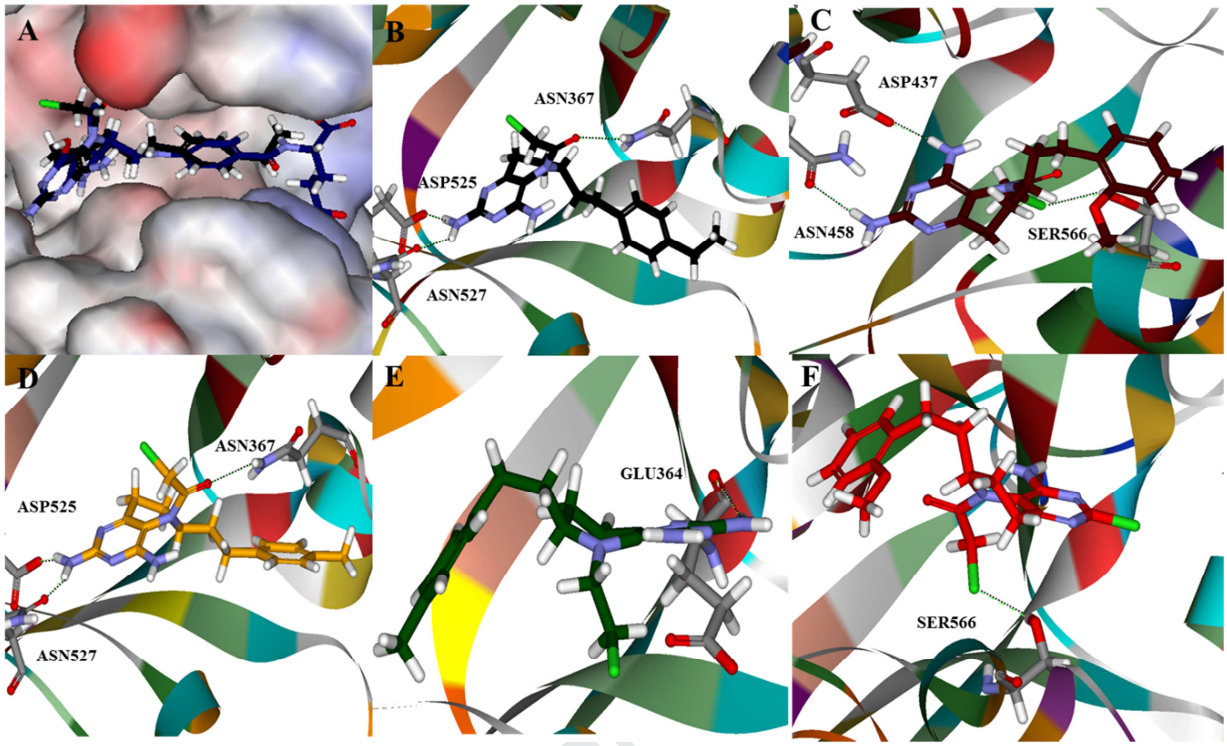

Figure 9. The homology model of the human MetH based on the crystal structure of *Thermotoga maritime* (PDB: 1Q8J) **A**) Overlay of the docked pose of compound **6c** (black) with MTHF (blue) in the homology model of the human MetH active site. **B**) Docked pose of compound **6c** (black). **C**) Docked pose of compound **6J** (deep red). **D**) Docked pose of compound $\mathbf{6a_5}$ (yellow). **E**) Docked pose of compound $\mathbf{6a_6}$ (green). **F**) Docked pose of compound $\mathbf{6J_2}$ (red).

3 CONCLUSION

MetH inhibitors represent a kind of new and promising chemotherapeutic agents. Based on the action mechanism of MetH and the previously reported inhibitors of the N^5-substituted tetrahydrofolate analogs, a novel series of N^5-substituted-6-substituted pyrido[3,2-*d*]pyrimidine antifolates as nonclassic antifolates were designed and tested for MetH inhibitory and antitumor activity. The structure-activity relationship for these compounds was summarized. We found that N^5-chloracetyl substitution compounds of substituted tetrahydrofolate analogs showed higher in vitro antiproliferative activity than others toward five cell lines including HL-60, HeLa, A549, H1299 and HT29 and compounds $\mathbf{6a_5}$, **6f**, and **6c** showed the highest activity against MetH (IC_{50}: 5.66 μM, 4.99 μM and 12.1 μM, respectively). The cell cycle distribution assay displayed that compound **6c** could increase the accumulation of G_1-phase cells. And compound **6c** showed highly potency in induction of apoptosis. Molecular modeling indicated that carbonyl of chloracetyl group played an important role in inhibition of MetH, which could interact with amino-acid residue Asn 367. This study revealed a new generation of lead compounds that could help in the design of

clinically useful MetH inhibitors with potential anticancer activity.

As the substrates for folate-dependent enzymes, including DHFR, TS, and MetH, shared a similar scaffold, antifolates always exhibited multi-targeted effects currently. And a sub-structure of this series were evaluated and revealed several compound series that possess the 2,4-diaminopyrido[3,2-*d*]pyrimidine substructure that inhibit, with varying potencies, DHFR. As a consequence, off-target activity, particularly those associated with antifolate, will be monitored in the future development of this compound class. It is foreseen that with further optimization, the MetH inhibitors will become novel antifolates to treat cancer.

4 EXPERIMENTAL SECTION

4.1. Chemistry

Reagents and solvents were purchased from common commercial suppliers and were used without further purification. The melting points of the synthesized compounds were determined with a SGW® X4 apparatus. ^{1}H NMR spectra were recorded at 400 MHz, and ^{13}C NMR were recorded at 100 MHz on a Bruker NMR spectrometer instrument. Tetramethylsilane was used as an internal standard to express the chemical shift in ppm: s, singlet; d, doublet; t, triplet; q, quartet; quin, quintet; m, multiplet; and bs, broad singlet. Mass spectra were recorded on Waters Xevo G2 Q-TOF mass spectrometer or Quattro Micro 2000. All target compounds were assessed for purity by Agilent Technologies 1260 Infinity HPLC system with an Extend-C18 column (4.6 mm × 150 mm, 3.5 μM). HPLC condition: methanol (CH_3OH): water (H_2O) =70: 30; flow rate, 1.0 mL/min; UV detection, from 210 to 280 nm; temperature, 25 ^{o}C; injection volume, 20 μL. The purities of target compounds were confirmed to be ≥95%. Thin-layer chromatography (TLC) was performed on silica-gel F254 plates. Compounds **4a**-**4j** were synthesized as previously reported [44, 45].

*4.1.1 General procedure for the synthesis of intermediates **5a-5j**.*

A solution of **4a** (100 mg, 0.36 mmol) and PtO_2 (10%) in ethanol (30 mL) was added to 1 mL 0.5 mol/L HCl in an autoclave. The autoclave was evacuated and backfilled with H_2 three times, pressurized to 0.4 Mpa, and stirred at room temperature for 12 h. The reaction mixture was filtered and the filtrate was adjusted to pH 7-8 with a saturated $NaHCO_3$ solution, and evaporated to dryness under reduced pressure. The resulting residue was purified by using a silica gel column (eluent: CH_2Cl_2/ CH_3OH, 9/1) to obtain **5a** as a white solid.

*4.1.1.1 6-(4-methylphenethyl)-5,6,7,8-tetrahydropyrido[3,2-d]pyrimidine-2,4-diamine (**5a**).*

Yield 92%, mp: 211-213 °C; ^{1}H NMR (400 MHz, DMSO-d_6) δ: 7.10 (q, J = 7.9 Hz, 4H), 6.06 (s, 2H), 5.20 (s, 2H), 3.69 (s, 1H), 2.95 (d, J = 5.7 Hz, 1H), 2.86-2.58 (m, 2H), 2.51-2.30 (m, 2H), 2.26 (s, 3H), 1.94-1.84 (m, 1H), 1.76-1.61 (m, 2H), 1.49-1.45 (m, 1H); ^{13}C NMR (100 MHz, DMSO-d_6) δ: 156.14, 155.53, 149.47, 145.63, 144.81, 139.57, 135.49, 134.92, 129.44, 129.31, 128.62, 122.84, 116.07, 111.94, 110.00, 106.68, 51.43, 37.89, 31.41, 28.45, 28.19, 21.08; ESI-TOF-MS: m/z calcd for $C_{16}H_{22}N_5$ [$(M+H)^+$], 284.18; found, 284.23.

*4.1.1.2 6-phenethyl-5,6,7,8-tetrahydropyrido[3,2-d]pyrimidine-2,4-diamine (**5b**).*

Yield 92%, mp: 183-184 °C; ^{1}H NMR (400 MHz, DMSO-d_6) δ: 7.50-7.00 (m, 5H), 6.00 (s, 2H), 5.16 (s, 2H), 3.69 (s, 1H), 2.97 (d, J = 6.3 Hz, 1H), 2.87-2.63 (m, 2H), 2.50-2.27 (m, 2H), 2.00-1.86 (m, 1H), 1.82-1.63 (m, 2H), 1.52-1.45 (m, 1H); ^{13}C NMR (100 MHz, DMSO-d_6) δ: 156.20, 155.52, 145.85, 142.75, 128.74, 126.10, 116.04, 51.48, 37.83, 31.87, 28.50, 28.21; HRMS (TOF ES$^+$): m/z calcd for $C_{15}H_{20}N_5$ [$(M+H)^+$], 270.1719, found, 270.1714.

*4.1.1.3 6-(4-ethylphenethyl)-5,6,7,8-tetrahydropyrido[3,2-d]pyrimidine-2,4-diamine (**5c**).*

Yield 90%, mp: 182-183 °C; ^{1}H NMR (400 MHz, DMSO-d_6) δ: 7.13 (q, J = 8.2 Hz, 4H), 6.19 (s, 2H), 5.32 (s, 2H), 3.76 (s, 1H), 2.96 (d, J = 6.9 Hz, 1H), 2.80-2.64 (m, 2H), 2.56 (q, J = 7.6 Hz, 2H), 2.48-2.32 (m, 2H), 1.94-1.85 (m, 1H), 1.84 -1.62 (m, 2H), 1.59-1.38 (m, 1H), 1.16 (t, J = 7.6 Hz, 3H); ^{13}C NMR (100 MHz, DMSO-d_6) δ: 155.81, 155.71, 144.65, 141.38, 139.84, 128.67, 128.11, 116.12, 51.38, 37.84, 31.42, 28.24, 28.11, 28.06, 16.18.

*4.1.1.4 6-(4-isopropylphenethyl)-5,6,7,8-tetrahydropyrido[3,2-d]pyrimidine-2,4-diamine (**5d**).*

Yield 94%, mp: 186-188 °C; ^{1}H NMR (400 MHz, $CDCl_3$) δ: 7.26 -7.06 (m, 4H), 4.85 (s, 2H), 4.53 (s, 2H), 3.07 (d, J = 6.1 Hz, 1H), 2.99-2.84 (m, 1H), 2.77 (t, J = 7.2 Hz, 2H), 2.64 (s, 2H), 2.16-2.02 (m, 2H), 1.85 (d, J = 6.7 Hz, 2H), 1.65-1.50 (m, 1H), 1.25 (d, J = 6.7 Hz, 6H); ^{13}C NMR (100 MHz, $CDCl_3$) δ: 157.13, 156.86, 151.04, 146.56, 139.19, 128.32, 126.51, 115.95, 52.24, 37.46, 33.70, 32.16, 28.89, 28.54, 24.07; ESI-TOF-MS: m/z calcd for $C_{18}H_{26}N_5$ [$(M+H)^+$], 312.22; found, 312.27.

*4.1.1.5 6-(4-(tert-butyl)phenethyl)-5,6,7,8-tetrahydropyrido[3,2-d]pyrimidine-2,4-diamine (**5e**).*

Yield 93%, mp: 247-249 °C; ^{1}H NMR (400 MHz, DMSO-d_6) δ: 7.30 (d, J = 8.3 Hz, 2H), 7.16 (d, J = 8.2 Hz, 2H), 6.53 (s, 2H), 5.63 (s, 2H), 3.92 (s, 1H), 2.98 (d, J = 6.9 Hz, 1H), 2.90-2.62 (m, 2H), 2.59-2.35 (m, 2H), 2.47-2.36 (m, 1H), 2.01-1.84 (m, 1H), 1.85-1.61 (m, 2H), 1.59-1.39 (m, 1H), 1.26 (s, 9H); ^{13}C NMR

(100 MHz, DMSO-d_6) δ: 156.24, 155.14, 148.34, 144.71, 139.52, 128.41, 125.45, 116.25, 51.24, 37.63, 34.51, 31.69, 31.24, 27.66, 27.11.

*4.1.1.6 6-(4-fluorophenethyl)-5,6,7,8-tetrahydropyrido[3,2-d]pyrimidine-2,4-diamine (**5f**).*

Yield 90%, mp: 215-217 °C; ^{1}H NMR (400 MHz, DMSO-d_6) δ 7.27 (dd, J = 8.1, 5.9 Hz, 2H), 7.10 (t, J = 8.8 Hz, 2H), 6.03 (s, 2H), 5.18 (s, 2H), 3.67 (s, 1H), 2.96 (d, J = 5.8 Hz, 1H), 2.86-2.63 (m, 2H), 2.50-2.30 (m, 2H), 1.89 (m, 1H), 1.71 (m, 2H), 1.48 (m, 1H); ^{13}C NMR (100 MHz, DMSO-d_6) δ: 162.19, 159.80, 156.25, 155.59, 145.94, 138.82, 130.46, 130.38, 116.00, 115.47, 115.26, 51.38, 30.97, 28.49, 28.22.

*4.1.1.7 6-(4-chlorophenethyl)-5,6,7,8-tetrahydropyrido[3,2-d]pyrimidine-2,4-diamine (**5g**).*

Yield 94%, mp: 172-174 °C; ^{1}H NMR (400 MHz, DMSO-d_6) δ: 7.34 (d, J = 8 Hz, 2H), 7.27 (d, J = 8.0 Hz, 2H), 6.26 (s, 2H), 5.40 (s, 2H), 3.78 (s, 1H), 2.96 (d, J = 5.9 Hz, 1H), 2.87-2.66 (m, 2H), 2.51-2.32 (m, 2H), 1.89 (d, J = 12.4 Hz, 1H), 1.81-1.63 (m, 2H), 1.48 (s, 1H); ^{13}C NMR (100 MHz, DMSO-d_6) δ: 155.91, 155.63, 141.76, 130.69, 130.65, 128.75, 128.66, 116.04, 51.26, 37.52, 31.08, 27.96, 27.86; HRMS (TOF ES$^+$): m/z calcd for $C_{15}H_{19}ClN_5$ [(M+H)$^+$], 304.1329; found, 304.1325.

*4.1.1.8 6-(4-methoxyphenethyl)-5,6,7,8-tetrahydropyrido[3,2-d]pyrimidine-2,4-diamine (**5h**).*

Yield 92%, mp: 186-188 °C; ^{1}H NMR (400 MHz, DMSO-d_6) δ: 7.15 (d, J = 8.6 Hz, 2H), 6.85 (d, J = 8.6 Hz, 2H), 6.66 (s, 2H), 6.01 (s, 2H), 3.72 (s, 3H), 3.02-2.92 (m, 1H), 2.83-2.57 (m, 2H), 2.50-2.37 (m, 1H), 1.87 (s, 3H), 1.80-1.55 (m, 2H), 1.54-1.35 (m, 1H); ^{13}C NMR (100 MHz, DMSO-d_6) δ: 157.82, 156.53, 154.59, 140.64, 134.44, 129.64, 116.20, 114.18, 55.42, 51.18, 37.81, 30.85, 27.50, 26.60; ESI-TOF-MS: m/z calcd for $C_{16}H_{22}N_5O$ [(M+H)$^+$], 300.18; found, 300.19.

*4.1.1.9 6-(3-methoxyphenethyl)-5,6,7,8-tetrahydropyrido[3,2-d]pyrimidine-2,4-diamine (**5i**).*

Yield 90%, mp: 196-198 °C; ^{1}H NMR (400 MHz, DMSO-d_6) δ: 7.19 (t, J = 8.0 Hz, 1H), 6.81 (d, J = 6.3 Hz, 2H), 6.74 (d, J = 8.4 Hz, 1H), 5.97 (s, 2H), 5.12 (s, 2H), 3.73 (s, 3H), 3.65 (s, 1H), 2.96 (d, J = 5.4 Hz, 1H), 2.84-2.63 (m, 2H), 2.49-2.31 (m, 2H), 1.90 (d, J = 12.8 Hz, 1H), 1.83-1.61 (m, 2H), 1.61-1.42 (m, 1H); ^{13}C NMR (100 MHz, DMSO-d_6) δ: 159.76, 156.38, 155.44, 146.36, 144.38, 129.72, 121.01, 116.02, 114.43, 111.51, 55.34, 51.51, 37.71, 31.93, 28.68, 28.29; HRMS (TOF ES$^+$): m/z calcd for $C_{16}H_{22}N_5O$ [(M+H)$^+$], 300.1824; found, 300.1820.

*4.1.1.10 6-(2-methoxyphenethyl)-5,6,7,8-tetrahydropyrido[3,2-d]pyrimidine-2,4-diamine (**5j**)*

Yield 92%, mp: 189-191 °C;^{1}H NMR (400 MHz, DMSO-d_6) δ: 7.17 (d, J = 5.7 Hz, 2H), 6.94 (d, J = 8.4

Hz, 1H), 6.87 (t, *J* = 7.3 Hz, 1H), 6.29 (s, 2H), 5.72 (s, 2H), 4.21 (s, 1H), 3.78 (s, 3H), 2.96 (d, *J* = 7.1 Hz, 1H), 2.80-2.60 (m, 2H), 2.50-2.31 (m, 2H), 1.98-1.89 (m, 1H), 1.79-1.56 (m, 2H), 1.55-1.40 (s, 1H); ^{13}C NMR (100 MHz, DMSO) δ 157.51, 130.39, 129.91, 127.55, 120.71, 116.11, 111.03, 63.40, 55.66, 51.53, 36.00, 27.76, 27.51, 26.39; ESI-TOF-MS: m/z calcd for $C_{16}H_{22}N_5O$ [$(M+H)^+$], 300.18; found, 300.29.

4.1.2 General procedure for the synthesis of title compounds ***6a$_5$, 6b-6j & 6j$_1$-6j$_3$.***

A solution of **5a** (100 mg, 0.35 mmol) in anhydrous DMF (3 mL) in an ice bath for 30 min was added to chloroacetyl chloride (100 μL, 1.26 mmol) and the reaction mixture was stirred for about 30 min. Then the mixture was extracted with CH_2Cl_2. The organic layers were combined, washed with saturated $NaHCO_3$ and water, dried over anhydrous Na_2SO_4, filtered, and concentrated. The residue was purified by column chromatography over silica gel, eluting with CH_2Cl_2/CH_3OH (30/1), to give **6a$_5$** as a white solid.

*4.1.2.1 6-(4-methylphenethyl)-5-chloracetyl-5,6,7,8-tetrahydropyrido[3,2-d]pyrimidine-2,4-diamine (**6a$_5$**).*

Yield 64%, mp: 159-160 °C; ^{1}H NMR (400 MHz, DMSO-d_6) *δ* 7.06 (s, 4H), 6.56 (s, 2H), 6.05 (s, 2H), 4.87-4.54 (m, 1H), 4.33-3.94 (m, 2H), 2.71-2.45 (m, 2H), 2.44-2.11 (m, 6H), 1.52-1.43 (m, 2H), 1.38-1.21 (m, 1H); ^{13}C NMR (100 MHz, DMSO-d_6) δ 167.04, 164.98, 161.54, 159.19, 139.40, 129.25, 128.64, 105.60, 52.31, 43.58, 36.95, 31.82, 29.58, 28.31, 21.08; HRMS (TOF ES$^+$): m/z calcd for $C_{18}H_{23}ClN_5O$ [$(M+H)^+$], 360.1591; found, 360.1582.

*4.1.2.2 6-phenethyl-5-chloracetyl-5,6,7,8-tetrahydropyrido[3,2-d]pyrimidine-2,4-diamine (**6b**).*

Yield 63%, mp: 166-168 °C; ^{1}H NMR (400 MHz, DMSO-d_6) *δ*: 7.25 (t, *J* = 7.3 Hz, 2H), 7.21-7.12 (m, 3H), 6.57 (s, 2H), 6.05 (s, 2H), 4.87-4.63 (m, 1H), 4.23-4.11 (m, 2H), 2.72-2.54 (m, 2H), 2.28-2.23 (m, 3H), 1.65-1.45 (m, 2H), 1.34-1.28 (m, 1H); ^{13}C NMR (100 MHz, DMSO-d_6) *δ*: 167.07, 165.64, 164.98, 162.63, 161.54, 160.81, 159.20, 150.86, 142.56, 140.48, 128.76, 128.68, 128.14, 126.11, 124.16, 105.59, 52.35, 43.59, 36.89, 32.28, 29.60, 28.31; HRMS (TOF ES$^+$): m/z calcd for $C_{17}H_{21}ClN_5O$ [$(M+H)^+$], 346.1435; found, 346.1435.

*4.1.2.3 6-(4-ethylphenethyl)-5-chloracetyl-5,6,7,8-tetrahydropyrido[3,2-d]pyrimidine-2,4-diamine (**6c**).*

Yield 65%, mp: 137-138 °C; ^{1}H NMR (400 MHz, DMSO-d_6) *δ*: 7.08 (s, 4H), 6.57 (s, 2H), 6.06 (s, 2H), 4.80-4.65 (m, 1H), 4.21-4.13 (m, 2H), 3.39-3.34 (m, 1H), 2.72-2.51 (m, 4H), 2.35-2.15 (m, 2H), 1.57-1.23 (m, 3H), 1.16-1.09 (m, 3H); ^{13}C NMR (100 MHz, DMSO-d_6) *δ*: 167.06, 164.92, 161.52, 159.21, 141.40, 139.69, 128.68, 128.06, 105.61, 65.39, 52.32, 43.59, 36.92, 31.85, 29.57, 28.23, 16.18; HRMS (TOF ES$^+$): m/z calcd for $C_{19}H_{25}ClN_5O$ [$(M+H)^+$], 374.1748; found, 374.1745.

*4.1.2.4 6-(4-isopropylphenethyl)-5-chloracetyl-5,6,7,8-tetrahydropyrido[3,2-d]pyrimidine-2,4-diamine (**6d**).*

Yield 63%, mp: 152-154 °C; ^{1}H NMR (400 MHz, DMSO-d_6) δ: 7.10 (s, 4H), 6.56 (s, 2H), 6.05 (s, 2H), 4.72 (s, 1H), 4.33-4.02 (m, 2H), 2.95-2.70 (m, 1H), 2.59 (s, 2H), 2.26 (s, 3H), 1.64-1.24 (m, 3H), 1.17 (d, J = 6.4 Hz, 6H); ^{13}C NMR (101 MHz, DMSO-d_6) δ: 167.06, 161.19, 159.22, 145.96, 140.18, 128.65, 126.56, 52.34, 43.59, 36.88, 33.49, 31.83, 29.54, 28.00, 24.44; HRMS (TOF ES$^+$): m/z calcd for $C_{20}H_{27}ClN_5O$ [(M+H)$^+$], 388.1904; found, 388.1900.

*4.1.2.5 6-(4-(tert-butyl)phenethyl)-5-chloracetyl-5,6,7,8-tetrahydropyrido[3,2-d]pyrimidine-2,4-diamine (**6e**).*

Yield 63%, mp: 151-153 °C;^{1}H NMR (400 MHz, DMSO-d_6) δ: 7.26 (d, J = 7.7 Hz, 2H), 7.10 (d, J = 7.9 Hz, 2H), 6.56 (s, 2H), 6.05 (s, 2H), 4.85-4.60 (m, 1H), 4.25-4.06 (m, 2H), 2.72-2.52 (m, 2H), 2.40-2.13 (m, 3H), 1.67-1.28 (m, 3H), 1.25 (s, 9H); ^{13}C NMR (100 MHz, DMSO-d_6) δ: 167.07, 164.88, 161.50, 159.22, 148.32, 139.43, 128.39, 125.39, 105.61, 52.32, 43.59, 36.82, 34.49, 31.68, 29.55, 28.24; HRMS (TOF ES$^+$): m/z calcd for $C_{21}H_{29}ClN_5O$ [(M+H)$^+$], 402.2061; found, 402.2058.

*4.1.2.6 6-(4-fluorophenethyl)-5-chloracetyl-5,6,7,8-tetrahydropyrido[3,2-d]pyrimidine-2,4-diamine (**6f**).*

Yield 64%, mp: 181-183 °C; ^{1}H NMR (400 MHz, DMSO-d_6) δ: 7.38-7.14 (m, 2H), 7.07 (t, J = 8.6 Hz, 2H), 6.58 (s, 2H), 6.06 (s, 2H), 4.85-4.58 (m, 1H), 4.28-3.98 (m, 2H), 2.74-2.51 (m, 2H), 2.35-2.16 (m, 3H), 1.52-1.43 (m, 2H), 1.41-1.21 (m, 1H); ^{13}C NMR (100 MHz, DMSO-d_6) δ: 167.09, 165.00, 161.53, 159.19, 138.63, 130.52, 130.44, 115.42, 115.21, 105.55, 52.23, 43.59, 36.96, 31.35, 29.61, 28.31; HRMS (TOF ES$^+$): m/z calcd for $C_{17}H_{20}ClFN_5O$ [(M+H)$^+$], 364.1340; found, 364.1331.

*4.1.2.7 6-(4-chlorophenethyl)-5-chloracetyl-5,6,7,8-tetrahydropyrido[3,2-d]pyrimidine-2,4-diamine (**6g**).*

Yield 62%, mp: 172-174 °C; ^{1}H NMR (400 MHz, DMSO-d_6) δ: 7.31 (d, J = 7.9 Hz, 2H), 7.22 (d, J = 8.1 Hz, 2H), 6.57 (s, 2H), 6.05 (s, 2H), 4.83-4.65 (m, 1H), 4.25-4.10 (m, 2H), 2.75-2.54 (m, 2H), 2.26 (s, 3H), 1.56-1.41 (m, 2H), 1.36-1.25 (s, 1H); ^{13}C NMR (100 MHz, DMSO-d_6) δ: 165.30, 161.56, 160.49, 159.18, 151.45, 141.58, 130.68, 128.60, 105.53, 52.22, 43.59, 36.68, 31.48, 29.62, 28.31; HRMS (TOF ES$^+$): m/z calcd for $C_{17}H_{20}Cl_2N_5O$ [(M+H)$^+$], 380.1045; found, 380.1039.

*4.1.2.8 6-(4-methoxyphenethyl)-5-chloracetyl-5,6,7,8-tetrahydropyrido[3,2-d]pyrimidine-2,4-diamine (**6h**).*

Yield 65%, mp: 144-145 °C; ^{1}H NMR (400 MHz, DMSO-d_6) δ: 7.09 (d, J = 7.8 Hz, 2H), 6.81 (d, J = 7.9 Hz, 2H), 6.66 (s, 2H), 6.14 (s, 2H), 4.90-4.50 (m, 1H), 4.32-3.96 (m, 2H), 3.70 (s, 3H), 2.80-2.41 (m, 3H),

2.40-2.09 (m, 2H), 1.85-1.20 (m, 3H); ^{13}C NMR (100 MHz, DMSO-d_6) δ: 167.07, 161.06, 159.32, 157.81, 134.36, 129.67, 129.59, 114.11, 105.73, 55.41, 52.25, 43.59, 36.97, 31.32, 29.44, 27.98; HRMS (TOF ES$^+$): m/z calcd for $C_{18}H_{23}ClN_5O_2$ [(M+H)$^+$], 376.1540; found, 376.1538.

*4.1.2.9 6-(3-methoxyphenethyl)-5-chloracetyl-5,6,7,8-tetrahydropyrido[3,2-d]pyrimidine-2,4-diamine (**6i**).*

Yield 60%, mp: 161-162 °C; ^{1}H NMR (400 MHz, DMSO-d_6) δ: 7.16 (t, J = 7.7 Hz, 1H), 6.76-6.71 (m, 3H), 6.58 (s, 2H), 6.06 (s, 2H), 4.87-4.62 (m, 1H), 4.21-4.13 (m, 2H), 3.72 (s, 3H), 2.70-2.52 (m, 2H), 2.39-2.13 (m, 3H), 1.53-1.45 (m, 2H), 1.34-1.29 (m, 1H); ^{13}C NMR (100 MHz, DMSO-d_6) δ: 167.09, 165.01, 163.80, 161.52, 161.36, 159.70, 159.57, 159.21, 144.17, 129.66, 121.00, 114.45, 112.10, 111.58, 105.59, 55.33, 52.31, 43.59, 36.78, 32.31, 29.60, 28.29; HRMS (TOF ES$^+$): m/z calcd for $C_{18}H_{23}ClN_5O_2$ [(M+H)$^+$], 376.1540; found, 376.15389

*4.1.2.10 6-(2-methoxyphenethyl)-5-chloracetyl-5,6,7,8-tetrahydropyrido[3,2-d]pyrimidine-2,4-diamine (**6j**).*

Yield 59%, mp: 147-149 °C; ^{1}H NMR (400 MHz, DMSO-d_6) δ: 7.20-7.09 (m, 2H), 6.91 (d, J = 8.0 Hz, 1H), 6.83 (t, J = 7.4 Hz, 1H), 6.54 (s, 2H), 6.06 (s, 2H), 4.81-4.65 (m, 1H), 4.31-4.05 (m, 2H), 3.74 (s, 3H), 2.62-2.49 (m, 2H), 2.38-2.15 (m, 3H), 1.70-1.21 (m, 4H); ^{13}C NMR (100 MHz, DMSO-d_6) δ: 167.05, 164.76, 161.49, 159.23, 157.44, 130.19, 130.08, 127.59, 120.64, 111.01, 105.69, 55.63, 52.49, 43.58, 34.95, 29.48, 28.21, 26.99; HRMS (TOF ES$^+$): m/z calcd for $C_{18}H_{23}ClN_5O_2$ [(M+H)$^+$], 376.1540; found, 376.1538.

*4.1.2.11 2,4-dimethoxy-6-(2-methoxyphenethyl)-5-chloracetyl-5,6,7,8-tetrahydropyrido[3,2-d]pyrimidine (**6j$_1$**).*

Yield 82%; ^{1}H NMR (400 MHz, $CDCl_3$) δ: 7.16 (t, J = 7.6 Hz, 1H), 7.12-7.00 (m, 1H), 6.86 (t, J = 7.4 Hz, 1H), 6.80 (d, J = 8.1 Hz, 1H), 4.98 (s, 1H), 4.17-3.96 (m, 8H), 3.74 (s, 3H), 2.79-2.67 (m, 2H), 2.66-2.52 (m, 2H), 2.47-2.30 (m, 1H), 1.82-1.47 (m, 3H); ^{13}C NMR (100 MHz, $CDCl_3$) δ: 166.82, 166.06, 164.42, 162.28, 157.30, 129.85, 127.23, 120.44, 112.78, 110.20, 55.12, 54.49, 52.43, 42.38, 33.31, 28.55, 27.89, 26.98, 14.43; HRMS (TOF ES$^+$): m/z calcd for $C_{20}H_{25}ClN_3O_4$ [(M+H)$^+$], 406.1534; found, 406.1534.

4.1.2.12

*2-chloro-4-amino-6-(2-methoxyphenethyl)-5-chloracetyl-5,6,7,8-tetrahydropyrido[3,2-d]pyrimidine (**6j$_2$**).*

Yield 63%, mp: 143-145 °C; ^{1}H NMR (400 MHz, $CDCl_3$) δ: 7.26-7.03 (m, 2H), 6.96-6.79 (m, 2H), 5.82-5.46 (d, 2H), 4.26-3.91 (m, 3H), 3.78 (s, 3H), 3.04-2.50 (m, 4H), 2.36 (d, J = 5.4 Hz, 1H), 2.13-1.46 (m, 3H); ^{13}C NMR (100 MHz, $CDCl_3$) δ: 165.26, 161.64, 159.78, 157.23, 156.64, 129.84, 128.17, 127.89, 120.81, 115.08, 110.66, 55.32, 54.49, 41.58, 31.32, 27.17, 26.71, 26.20; HRMS (TOF ES$^+$): m/z calcd for $C_{18}H_{21}Cl_2N_4O_2$ [(M+H)$^+$], 395.1042; found, 395.1041.

4.1.2.13

*2-methoxy-4-amino-6-(2-methoxyphenethyl)-5-chloracetyl-5,6,7,8-tetrahydropyrido[3,2-d]pyrimidine (**6j$_3$**).*

Yield 60%, mp: 46-48 °C; ^{1}H NMR (400 MHz, $CDCl_3$) δ: 7.26-7.01 (m, 2H), 7.01-6.65 (m, 2H), 5.31 (s, 1H), 5.07-4.72 (m, 1H), 4.39-3.52 (m, 7H), 2.97-2.23 (m, 5H), 2.02-1.29 (m, 4H); ^{13}C NMR (100 MHz, $CDCl_3$) δ: 132.36, 130.93, 129.88, 128.85, 127.77, 127.44, 120.73, 110.55, 110.47, 71.81, 55.27, 54.67, 53.53, 42.44, 41.76, 34.40, 31.51, 30.71, 29.70, 29.45, 28.24, 27.72, 27.48, 26.80, 26.22; HRMS (TOF ES$^+$): m/z calcd for $C_{19}H_{24}ClN_4O_3$ [(M+H)$^+$], 391.1537; found, 391.1540.

*4.1.3 6-(4-methylphenethyl)-5-formyl-5,6,7,8-tetrahydropyrido[3,2-d]pyrimidine-2,4-diamine (**6a$_1$**).*

A solution of **5a** (50 mg, 0.17 mmol) in 10 mL CH_2Cl_2 was added formic acid (0.5 mL) and the mixture was at room temperature stirred for 1 h. Then acetic anhydride (0.5 mL) was added and the resulting solution was stirred for 0.5 h. The mixture was adjusted to pH 7 with a saturated $NaHCO_3$ solution and extracted with CH_2Cl_2. The organic layer was separated, dried over anhydrous Na_2SO_4, filtered, and concentrated. The residue was purified by column chromatography over silica gel, eluting with CH_2Cl_2/CH_3OH (9/1), to give **6a$_1$** as a white solid. Yield 91%, mp: 150-152 °C; ^{1}H NMR (400 MHz, DMSO-d_6) δ: 8.20&8.07 (s, 1H), 7.11-6.99 (m, 4H), 6.45 (s, 1H), 6.91 (s, 3H), 4.62-4.49&4.05-3.91 (m, 1H), 2.64-2.40 (m, 3H), 2.41-2.30 (m, 1H), 2.24 (s, 3H), 2.16-1.96 (m, 1H), 1.83-1.48 (m, 3H); ^{13}C NMR (100 MHz, DMSO-d_6) δ: 161.47, 161.11, 160.67, 160.53, 159.18, 158.98, 158.94, 141.57, 141.42, 139.60, 139.10, 128.72, 128.63, 128.18, 128.06, 53.66, 48.29, 34.24, 33.53, 31.74, 31.67, 28.47, 28.22, 27.87, 27.03, 26.51, 21.55, 16.16; ESI-TOF-MS: m/z calcd for $C_{17}H_{22}N_5O$ [(M+H)$^+$], 312.18; found, 312.28.

*4.1.4 6-(4-methylphenethyl)-5-acryloyl-5,6,7,8-tetrahydropyrido[3,2-d]pyrimidine-2,4-diamine (**6a$_2$**).*

A solution of **5a** (100 mg, 0.35 mmol) and 20 mg $NaHCO_3$ in anhydrous DMF (3 mL) was added to acryloyl chloride (100 μL, 1.24 mmol) and the reaction mixture was at room temperature stirred for about 30 min. Then the mixture was extracted with CH_2Cl_2. The organic layers were combined, washed with saturated $NaHCO_3$ and water, dried over anhydrous Na_2SO_4, filtered, and concentrated. The residue was

purified by column chromatography over silica gel, eluting with CH_2Cl_2/CH_3OH (30/1), to give **6a$_2$** as a white solid. Yield 58%, mp: 207-209 °C; ^{1}H NMR (400 MHz, DMSO-d_6) δ: 7.12-7.01 (m, 4H), 6.38 (s, 2H), 6.31-6.14 (m, 2H), 6.00 (s, 2H), 5.70-5.57 (m, 1H), 5.06-4.60 (m, 1H), 2.66-2.48 (m, 2H), 2.35-2.08 (m, 6H), 1.68-1.33 (m, 3H); ^{13}C NMR (100 MHz, DMSO-d_6) δ: 165.68, 163.45, 161.28, 159.69, 139.49, 134.89, 129.79, 129.22, 128.68, 127.93, 106.29, 51.36, 36.62, 31.88, 29.47, 28.09, 21.08; HRMS (TOF ES$^+$): m/z calcd for $C_{19}H_{24}N_5O$ [$(M+H)^+$], 338.1981; found, 338.1988.

*4.1.5 6-(4-methylphenethyl)-5-allyl-5,6,7,8-tetrahydropyrido[3,2-d]pyrimidine-2,4-diamine (**6a$_3$**).*

A solution of **5a** (100 mg, 0.35 mmol) and 111 mg K_2CO_3 in anhydrous DMF (5 mL) was added to allyl bromide (70 μL, 1.04 mmol) and the reaction mixture was at room temperature stirred for 48 h. Then the mixture was extracted with CH_2Cl_2. The organic layers were combined, washed with water, dried over anhydrous Na_2SO_4, filtered, and concentrated. The residue was purified by column chromatography over silica gel, eluting with CH_2Cl_2/CH_3OH (30/1), to give **6a$_3$** as a white solid. Yield 60%, mp: 69-71 ^{o}C; ^{1}H NMR (400 MHz, DMSO-d_6) δ: 7.03 (s, 4H), 6.16-5.99 (m, 1H), 5.90 (s, 2H), 5.51 (s, 2H), 5.21 (d, J = 17.1 Hz, 1H), 5.10 (d, J = 10.1 Hz, 1H), 3.39-3.31 (m, 1H), 3.18-3.05 (m, 1H), 2.91 (d, J = 2.9 Hz, 1H), 2.74-2.61 (m, 1H), 2.56-2.45 (m, 1H), 2.47 (s, 1H), 2.40-2.26 (m, 2H), 2.23 (s, 3H), 2.15-1.99 (m, 1H), 1.53-1.34 (m, 3H); ^{13}C NMR (100 MHz, DMSO-d_6) δ: 160.37, 158.76, 153.93, 139.79, 137.76, 134.77, 129.19, 128.63, 117.15, 116.20, 56.25, 52.44, 33.58, 32.18, 24.98, 21.06, 19.79; HRMS (TOF ES$^+$): m/z calcd for $C_{19}H_{26}N_5$ [$(M+H)^+$], 324.2188; found, 324.2184.

*4.1.6 6-(4-methylphenethyl)-5-cyclopropionyl-5,6,7,8-tetrahydropyrido[3,2-d]pyrimidine-2,4-diamine (**6a$_4$**).*

A solution of**5a** (100 mg, 0.35 mmol) and 16 mg K_2CO_3 in anhydrous DMF (3 mL) was added to isopropanecarbonyl chloride (100 μL, 1.10 mmol) and the reaction mixture was at room temperature stirred for 30 min. Then the mixture was extracted with CH_2Cl_2. The organic layers were combined, washed with saturated $NaHCO_3$ and water, dried over anhydrous Na_2SO_4, filtered, and concentrated. The residue was purified by column chromatography over silica gel, eluting with CH_2Cl_2/CH_3OH (30/1), to give **6a$_4$** as a white solid. Yield 63%, mp: 90-92 °C; ^{1}H NMR (400 MHz, DMSO-d_6) δ: 7.05 (s, 4H), 6.38 (s, 2H), 5.97 (s, 2H), 4.87-4.66 (m, 1H), 2.64-2.50 (m, 2H), 2.33-2.19 (m, 5H), 2.20-2.09 (m, 1H), 1.65-1.30 (m, 4H), 0.98-0.87 (m, 1H), 0.80-0.51 (m, 3H); ^{13}C NMR (100 MHz, DMSO-d_6) δ: 173.86, 163.14, 161.18, 159.99,

139.50, 134.87, 129.21, 128.66, 107.09, 51.20, 36.51, 31.99, 29.40, 28.00, 21.08, 12.44, 8.49, 8.35; HRMS (TOF ES^+): m/z calcd for $C_{20}H_{26}N_5O$ [$(M+H)^+$], 352.2137; found, 352.2139.

*4.1.7 6-(4-methylphenethyl)-5-(2-chloroethyl)-5,6,7,8-tetrahydropyrido[3,2-d]pyrimidine-2,4-diamine (**6a$_6$**).*

A solution of **6a$_5$** (50 mg, 0.14 mmol) and BH_3-THF (1 mL, 1 mol/L) in anhydrous THF (1 mL) was at room temperature stirred overnight. The mixture was added 20% HCl and stirred for 1 h. Then the mixture was adjusted to pH 7 with a saturated $NaHCO_3$ solution, and evaporated to dryness under reduced pressure. The residue was purified by column chromatography over silica gel, eluting with CH_2Cl_2/CH_3OH (30/1), to give **6a$_6$** as a white solid. Yield 75%, mp: 152-154 °C;^{1}H NMR (400 MHz, DMSO-d_6) δ: 7.22-6.87 (m, 4H), 6.32 (s, 2H), 5.84 (s, 2H), 4.02-3.89 (m, 1H), 3.82-3.64 (m, 1H), 3.09-2.81 (m, 3H), 2.78-2.63 (m, 1H), 2.63-2.50 (m, 1H), 2.42-2.29 (m, 2H), 2.24 (s, 3H), 2.14-2.01 (m, 1H), 1.57-1.40 (m, 3H). ^{13}C NMR (100 MHz, DMSO-d_6) δ: 160.57, 157.94, 139.72, 134.87, 129.30, 128.51, 115.67, 54.45, 52.76, 43.79, 33.22, 32.18, 29.67, 24.24, 21.06. HRMS (TOF ES^+): m/z calcd for $C_{18}H_{25}ClN_5$ [$(M+H)^+$], 346.1798; found, 346.1796.

*4.1.8 6-(4-methylphenethyl)-5-(3-chloropropionyl)-5,6,7,8-tetrahydropyrido[3,2-d]pyrimidine-2,4-diamine (**6a$_7$**).*

A solution of **5a** (100 mg, 0.35 mmol) in anhydrous DMF (3 mL) was added to bromoacetyl bromide (100 μL, 1.15 mmol) and the reaction mixture was at room temperature stirred for 30 min. Then the mixture was extracted with CH_2Cl_2. The organic layers were combined, washed with saturated $NaHCO_3$ and water, dried over anhydrous Na_2SO_4, filtered, and concentrated. The residue was purified by column chromatography over silica gel, eluting with CH_2Cl_2/CH_3OH (30/1), to give **6a$_7$** as a white solid. Yield 51%, mp: 151-153 °C; ^{1}H NMR (400 MHz, $CDCl_3$) δ: 7.20-7.01 (m, 4H), 5.20-4.90 (m, 3H), 4.73 (s, 1H), 3.98-3.67 (m, 2H), 3.07-2.12 (m, 11H), 1.98-1.54 (m, 3H); ^{13}C NMR (100 MHz, $CDCl_3$) δ: 171.20, 129.40, 129.16, 128.24, 52.58, 40.32, 36.62, 32.58, 31.42, 29.92, 28.30, 20.98; HRMS (TOF ES^+): m/z calcd for $C_{19}H_{25}ClN_5O$ [$(M+H)^+$], 374.1748; found, 374.1749.

*4.1.9 6-(4-methylphenethyl)-5-(3-chloropropyl)-5,6,7,8-tetrahydropyrido[3,2-d]pyrimidine-2,4-diamine (**6a$_8$**).*

A procedure similar to the preparation of **6a$_6$** was followed to prepare **6a$_7$** from **3a$_8$**. The yield was 73% as a colorless oil; ^{1}H NMR (400 MHz, DMSO-d_6) δ: 7.05 (s, 4H), 6.68 (s, 2H), 6.35 (s, 2H), 3.79-3.61 (m,

2H), 3.43-3.30 (m, 3H), 2.99 (s, 1H), 2.84-2.53 (m, 4H), 2.47-2.34 (s, 2H), 2.24 (s, 3H), 2.23-1.81 (m, 3H). ^{13}C NMR (100 MHz, DMSO-d_6) δ: 161.47, 156.39, 156.01, 139.62, 134.86, 129.24, 128.61, 116.69, 61.19, 52.55, 50.67, 44.04, 33.31, 32.09, 31.33, 29.66, 21.07; HRMS (TOF ES$^+$): m/z calcd for $C_{19}H_{27}ClN_5$ [(M+H)$^+$], 360.1955; found, 360.1961.

*4.1.10 6-(4-methylphenethyl)-5-bromoacetyl-5,6,7,8-tetrahydropyrido[3,2-d]pyrimidine-2,4-diamine (**6a$_9$**).*

A solution of **5a** (100 mg, 0.35 mmol) in anhydrous DMF (3 mL) was added to bromoacetyl bromide (100 μL, 1.15 mmol) and the reaction mixture was stirred for about 30 min. Then the mixture was extracted with CH_2Cl_2. The organic layers were combined, washed with saturated $NaHCO_3$ and water, dried over anhydrous Na_2SO_4, filtered, and concentrated. The residue was purified by column chromatography over silica gel, eluting with CH_2Cl_2/CH_3OH (30/1), to give **6a$_9$** as a white solid. Yield 49%, mp: 196-198 °C; ^{1}H NMR (400 MHz, DMSO-d_6) δ: 7.33-6.90 (m, 6H), 4.90-4.55 (m, 1H), 4.33-3.76 (m, 2H), 2.77-2.52 (m, 2H), 2.45-2.35 (d, J = 6.5 Hz, 1H), 2.25 (s, 3H), 2.24-1.90 (m, 2H), 1.83-2.40 (m, 3H); ^{13}C NMR (100 MHz, DMSO-d_6) δ: 160.05, 153.57, 138.60, 135.13, 129.30, 129.25, 128.64, 128.55, 47.68, 31.95, 31.42, 30.13, 28.83, 26.42, 21.08. HRMS (TOF ES$^+$): m/z calcd for $C_{18}H_{23}BrN_5O$ [(M+H)$^+$], 404.1086, 406.1066; found, 404.1089, 406.1070.

4.2 Evaluation of Cell Viability.

The 3-(4,5-dimethylthiazol-2-yl)-5-(3-carboxymethoxyphenyl)-2-(4-sulfophenyl)-2H-tetrazolium (MTS) assay was used to determine the in vitro antiproliferative effect of the compounds. HL-60, HeLa, A549, H1299 and HT29 cells were cultured in 96-well plates at an initial density of 1×10^3 cells/well, 1×10^3 cells/well, 2×10^3 cells/well, 1×10^3 cells/well and 3×10^3 cells/well in RPMI-1640 supplemented with 10% fetal bovine serum, penicillinestreptomycin solution, at 37 ^{o}C with 5% CO_2. Cells were grown for 12 h and then treated with compounds at concentrations ranging from 0.0078 μM to 100 μM and incubated for 24, 48 or 72 h in 200 μL media. MTS reagent (20 μL) in phosphate buffer solution was added to each well and incubated further for 3-4 h. A490 nm was measured using a 96-well plate spectrophotometer (BioRad Benchmark plus). Three individual experiments were performed to obtain mean cell viability. MTX was used as positive controls.

4.3 MetH activity assay.

HL-60 cells at the density of 1×10^6 cells/well (900 μL) in 24-well plates were cultured overnight before treating with various concentrations of test compounds (100 μL) for 3 h. Then the cells were harvested

(1,000 rmp, 10 min) and lysed with lysis buffer (150 μL). After centrifugation (10,000 rpm, 10 min, at 4 ^{o}C), the supernatants were assayed in EP tubes for MetH activity. The assay solution contained 93 μL deionized water, 20 μL 1 mol/L PBS (pH 7.2), 5 μL 1 mol/L DTT, 5 μL 0.76 mmol/L SAM, 5 μL 20 mmol/L Hcy, 20 μL 0.5 mmol/L OH-Cbl. After adding 40 μL cell lysates into the mixture, it was preincubated at 37 ^{o}C for 5 min immediately. Then the reaction was initiated by mixing with 12 μL 4.2 mmol/L MTHF and incubated 37 ^{o}C for 10 min. The reaction was terminated by the addition of 50 μL stop buffer (5 mmol/L HCl+51% formic acid) and incubated at 80 ^{o}C for 10 min. After cooling, 200 μl mixture was transferred to 96-well microplates. Then the plate was read at 350 nm by using a 96-well plate spectrophotometer (BioRad Benchmark plus).

4.4 Cell Cycle Assay.

HL-60 cells at a density of 0.8×10^{6} cells per well were cultured in 60 mm petri dish overnight, then they were harvested and washed twice with ice-cold PBS after treating with compound **6c** (0.5 μM and 0.75 μM) or 0.1% DMSO for 24 h. Then, these cells were fixed in 70% cooled ethanol at 4 ºC overnight, until being washing with PBS just before analysis by flow cytometry. 0.5 mL PBS within 10 mg/mL RNase A was added to the fixed cells and incubated at 37 ^{o}C for 30 min in the dark. After this, 10 μL propidium iodide (PI) was added to the cells. The DNA contents were determined by a flow cytometry using the BD FACSCalibur flow cytometer.

4.5 Apoptosis Analysis.

HL-60 cells at a density of 0.5×10^{6} cells per well were cultured in 60 mm petri dish overnight, then they were harvested and washed twice with ice-cold PBS after treating with compound **6c** (0.5 μM and 0.75 μM) or 0.1% DMSO for 48 h. 400 μL BindingBuffer with 5 μL AnnexinV-FITC was add to the cells and incubated for 15 min at room temperature in the dark. After this, 10 μL PI was added to the cells and incubated for 5 min. Cells were assayed for apoptosis by flow cytometry using the BD FACSCalibur flow cytometer.

4.6 Molecular Modeling Computational Studies.

Multiple sequences of human, rat, and *Thermotoga maritime* methionine synthases (MS) were used in the alignment process. The multiple sequence alignment obtained in the previous step was used together with the crystal structure of *Thermotoga maritime* MS (PDB: 1Q8J) as an input for the building of the homology model of the human MetH using Accelrys Discovery Studio client 2.5 (DS 2.5) software. The

protonation state of the proteins and the ligands were calculated using the default settings. Water molecules in the active site were removed. The active site was defined by a sphere of 10.0 Å from the native ligand in the homology model of the human MetH. The CDocker protocol was used to score the docked poses.

SUPPORTING INFORMATION

The Supporting Information is available free of charge on the ACS Publications Web site at The Supporting Information is available free of charge on the ACS Publications website at DOI:

Synthesis and characterization of **5j$_1$-5j$_3$**. Copies of HRMS, ^{1}H NMR and ^{13}C NMR spectra of final compounds (PDF). Docking. HPLC traces of key target compound **6c**.

AUTHOR INFORMATION

Corresponding Author

$^{\perp}$J.Y.L. and Z.L.Z. E-mail: jyliu@bjmu.edu.cn and lilybmu@bjmu.edu.cn

Author Contributions

*M.W. and C.T. contributed equally to this work and are considered as co-first authors.

ACKNOWLEDGMENTS

The authors thank the Peking University Medical and Health Analysis Center for their help on the cell cycle assay and apoptosis analysis. This work was supported by the National Natural Science Foundation of China (21172014).

ABBREVIATIONS USED

DHFR, dihydrofolate reductase; TS, thymidylate systhase; THF, tetrahydrofuran; DMF, *N*,*N*-dimethylformamide; DMAC, dimethylacetamide; rt, room temperature; MTX, methotrexate; PBS, phosphate buffer saline; DTT, Dithiothreitol; SAM, s-adenosyl methionine; Hcy, homocysteine; OH-Cbl, hydroxocobalamin; PDB, protein data bank

REFERENCES

[1] J. Hu, B. Wang, N. R. Sahyoun, Application of the key events dose-response framework to folate metabolism, Crit. Rev. Food Sci. 56 (2016) 1325-1333.

[2] J. Stubbe, Binding site revealed of nature's most beautiful cofactor, Science 266 (1994) 1663-1664.

[3] R. Banerjee, S. W. Ragsdale, The Many faces of vitamin B_{12}: catalysis by cobalamin-dependent enzymes, Annu. Rev. Biochem. 72 (2003) 209-247.

[4] R. G. Matthews, Cobalamin-dependent methyltransferases, Acc. Chem. Res. 34 (2001) 681-689.

[5] N. Kumar, M. Jaworska, P. Lodowski, Electronic structure of cofactor-substrate reactant complex involved in the methyl transfer reaction catalyzed by cobalamin-dependent methionine synthase, J. Phys. Chem. B 115 (2011) 6722-6731.

[6] C. G. Julio, V. B. Ruma, H. Sha, Comparison of cobalamin-independent and cobalamin-dependent methionine synthases from *Escherichia coli*: two solutions to the same chemical problem, Biochemistry 31 (1992) 6045-6056.

[7] S. Ravanel, M. A. Block, P. Rippert, Methionine metabolism in plants: chloroplasts are autonomous for *de novo* methionine synthesis and can import S-adenosylmethionine from the cytosol, J. Biol. Chem. 279 (2004) 22548-22557.

[8] M. M. Kacprzak, I. Lewandowska, R. G. Matthews, Transcriptional regulation of methionine synthase by homocysteine and choline in Aspergillus nidulans, Biochem. J. 376 (2003) 517-524.

[9] I. Ifergan, Y. G. Assaraf, Molecular mechanisms of adaptation to folate deficiency, Vitam. Horm. 79 (2008) 99-143.

[10] S. Datta, M. Koutmos, K. A. Pattridge, A disulfide-stabilized conformer of methionine synthase reveals an unexpected role for the histidine ligand of the cobalamin cofactor, PNAS 105 (2008) 4115-4120.

[11] A. C. Newman, O. D. K Maddocks, One-carbon metabolism in cancer, Brit. J. Cancer 116 (2017) 1499-1504.

[12] S. C. Kalhan, One carbon metabolism in pregnancy: Impact on maternal, fetal and neonatal health, Mol. Cell Endocrinol. 435 (2016) 48-60.

[13] I. M. Kompis, K. T. Islam, L. Rudolf, DNA and RNA synthesis: antifolates, Chem. Rev. 105 (2006) 593-620.

[14] J. D. Finkelstein, Methionine metabolism in mammals, J. Nutr. Biochem. 1 (1990) 228-237.

[15] V. Pavillard, A. Nicolaou, J. A. Double, Methionine dependence of tumours: a biochemical strategy for optimizing paclitaxel chemosensitivity in vitro, Biochem. Pharmacol. 71 (2006) 772-778.

[16] M. Wang, J. J. Yang, L. M. Xue, Progress in the studies on methionine synthase inhibitors, Chin. J. Med. Chem. 6 (2017) 466-476.

[17] T. Fiskerstrand, P. M. Ueland, H. Refsum, Response of the methionine synthase system to short-term culture with homocysteine and nitrous oxide and its relation to methionine dependence, Int. J. Cancer 72 (1997) 301-306.

[18] A. Nicolaou, S. H. Kenyon, J. M. Gibbons, In vitro inactivation of mammalian methionine synthase by nitric oxide, Eur. J. Clin. Invest. 26 (1996) 167-170.

[19] M. Brouwer, W. Chamulitrat, G. Ferruzzi, Nitric oxide interactions with cobalamins: biochemical and functional consequences, Blood (88) 1996, 1857-1864.

[20] A. Nicolaou, C. J. Waterfield, S. H. Kenyon, The inactivation of methionine synthase in isolated rat hepatocytes by sodium nitroprusside, Eur. J. Biochem. 244 (1997) 876-882.

[21] A. J. Barak, H. C. Beckenhauer, D. J. Tuma, Methionine synthase-a possible prime site of the ethanolic lesion in liver, Alcohol 26 (2002) 65-67.

[22] J. R. Smith, J. G. Smith, Effects of methylmercury in vitro on methionine synthase activity in various rat tissues, Bull. Environ. Contam. Toxicol. 45 (1990) 649-654.

[23] S. P. Stabler, E. P. Brass, P. D. Marcell, Inhibition of cobalamin-dependent enzymes by cobalamin analogues in rats, J. Clin. Invest. 87 (1991)1422-1430.

[24] T. Bito, Y. Yabuta, T. Ichiyanagi, A dodecylamine derivative of cyanocobalamin potently inhibits the activities of cobalamin-dependent methylmalonyl-CoA mutase and methionine synthase of *Caenorhabditis elegans*, Febs Open Bio 4 (2014) 722-729.

[25] T. Bito, M. Yasui, T. Iwaki, Dodecylamine derivative of hydroxocobalamin acts as a potent inhibitor of cobalamin-dependent methionine synthase in mammalian cultured COS-7 cells, Food Nutr. Sci. 5 (2014) 1318-1325.

[26] E. C. Banks, S. W. Doughty, S. M. Toms, Inhibition of cobalamin-dependent methionine synthase by substituted benzo-fused heterocycles, FEBS J. 274 (2007) 287-299.

[27] H. Elshihawy, M. A. Helal, M. Said, Design, synthesis, and enzyme kinetics of novel benzimidazole and quinoxaline derivatives as methionine synthase inhibitors, Bioorg. Med. Chem. 22 (2014) 550-558.

[28] I. M. Elfekki, W. F. Hassan, H. E Elshihawy, Molecular modeling studies and synthesis of novel methyl 2-(2-(4-oxo-3-aryl-3,4-dihydroquinazolin-2-ylthio)acetamido)alkanoates with potential anti-cancer activity as inhibitors for methionine synthase, Chem. Pharm. Bull. 62 (2014) 675-694.

[29] Z. L. Zhang, C. Tian, S. X. Zhou, Mechanism-based design, synthesis and biological studies of N^5-substituted tetrahydrofolate analogs as inhibitors of cobalamin-dependent methionine synthase and potential anticancer agents, Eur. J. Med. Chem. 58 (2012) 228-236.

[30] X. L. Deng, Y. Guo, C. Tian, Design, synthesis and activities of aziridine derivatives of

N^5-methyltetrahydrofolate against methionine synthase, Chem. Res. Chin. Univ. 31 (2015) 742-745.

[31] L. Wang, A. Wallace, S. Raghavan, 6-Substituted pyrrolo[2,3-*d*]pyrimidine thienoyl regioisomers as targeted antifolates for folate receptor α and the proton-coupled folate transporter in human tumors, J. Med. Chem. 58 (2015) 6938-6959.

[32] L. Golani, C. George, S. Zhao, Structure-activity profiles of novel 6-substituted pyrrolo[2,3-*d*]pyrimidine thienoyl antifolates with modified amino acids for cellular uptake by folate receptors α and β and the proton-coupled folate transporter, J. Med. Chem. (57) 2014 8152-8166.

[33] K. R. Fales, F. G. Njoroge, H. B. Brooks, Discovery of *N*-(6-fluoro-1-oxo-1,2-dihydroisoquinolin-7-yl)-5-[(3R)-3-hydroxypyrrolidin-1-yl]thiophene-2-sulfonamide (LSN 3213128), a potent and selective nonclassical antifolate aminoimidazole-4-carboxamide ribonucleotide formyltransferase (AICARFT) inhibitor effective at tumor suppression in a cancer xenograft model, J. Med. Chem. 60 (2017) 9599-9616.

[34] L. K. Golani, A. Wallace-Povirk, S. M. Deis, Tumor targeting with novel 6-substituted pyrrolo [2,3-*d*] pyrimidine antifolates with heteroatom bridge substitutions via cellular uptake by folate receptor α and the proton-coupled folate transporter and inhibition of de novo purine nucleotide biosynthesis, J. Med. Chem. 59 (2016) 7856-7876.

[35] S. Raz, M. Stark, Y. G. Assaraf, Folylpoly-γ-glutamate synthetase: A key determinant of folate homeostasis and antifolate resistance in cancer, Drug Resistance Updates 28 (2016) 43-64.

[36] N. Gonen, Y. G. Assaraf, Antifolates in cancer therapy: Structure, activity and mechanisms of drug resistance, Drug Resistance Updates 15 (2012) 183-210.

[37] A. Gangjee, A. P. Vidwans, A. Vasudevan, Structure-based design and synthesis of lipophilic 2,4-diamino-6-substituted quinazolines and their evaluation as inhibitors of dihydrofolate reductases and potential antitumor agents, J. Med. Chem. 41 (1998) 3426-3434.

[38] D. C. Chan, H. Fu, R. A. Forsch, Design, synthesis, and antifolate activity of new analogues of piritrexim and other diaminopyrimidine dihydrofolate reductase inhibitors with ω-carboxyalkoxy or ω-carboxy-1-alkynyl substitution in the side chain, J. Med. Chem. 48 (2005) 4420-4431.

[39] J. R. Piper, C. A. Johnson, J. A. Maddry, Studies on analogues of classical antifolates bearing the naphthoyl group in place of benzoyl in the side chain, J. Med. Chem. 36 (1993) 4161-4171.

[40] R. L. Kisliuk, Deaza analogs of folic acid as antitumor agents, Curr. Pharm. Des. 9 (2003) 2615-2625.

[41] F. M .Sirotnak, J. I. DeGraw, D. M. Moccio, New folate analogs of the 10-deazaaminopterin series. Basis for structural design and biochemical and pharmacologic properties, Cancer Chemother. Pharmacol. 12 (1984) 18-25.

[42] C. Tian, Z. L. Zhang, S. X. Zhou, Synthesis, antifolate and anticancer activities of N^5-substituted 8,10-dideazatetrahydrofolate analogues, Chem. Biol. Drug Des. 87 (2016) 444-454.

[43] C. Tian, Z. L. Zhang, J. Y. Liu, Synthesis and evaluation of 8-deaza-5,6,7,8-tetrahydromethotrexate derivatives as dihydrofolate reductase inhibitors, J. Chin. Pharm. Sci. 21 (2012) 142-148.

[44] M. Wang, C. Tian, X. W. Wang, A convenient one-pot process for the synthesis of 2,4-dihydroxy-6-phenylethylenyl-8-deazapteridine derivatives, Tetrahedron 72 (2016) 2742-2747.

[45] M Wang, J. J. Yang, M. M. Yuan, Synthesis and antiproliferative activity of a series of novel 6-substituted pyrido[3,2-*d*]pyrimidines as potential nonclassical lipophilic antifolates targeting dihydrofolate reductase, Eur. J. Med. Chem. 128 (2017) 88-97.

[46] J. Walling, From methotrexate to pemetrexed and beyond. A review of the pharmacodynamic and clinical properties of antifolates, Invest. New Drug 24 (2006) 37-77.

[47] C. Tian, M. Wang, Z. F Han, Design, synthesis and biological evaluation of novel 6-substituted pyrrolo[3,2-*d*] pyrimidine analogues as antifolate antitumor agents, Eur. J. Med. Chem. 138 (2017) 630-643.

[48] R. Ralhan, J. Kaur, Alkylating agents and cancer therapy, Expert Opin. Ther. Patents, 17 (2007) 1061-1075.

[49] C. Tang, Z. L. Zhang, B. Xu, Two newly synthesized 5-methyltetrahydrofolate-like compounds inhibit methionine synthase activity accompanied by cell cycle arrest in G_1/S phase and apoptosis in vitro, Anti-Cancer Drug 19 (2008) 697-704.

Highlight

- A series of N^5-substituted tetrahydropteroate analogs were efficiently synthesized.
- Compounds were evaluated for *in vitro* MetH inhibition and antitumor activity.
- Compound **6a**$_5$, **6c**, **6e**, **6f** and **6g** showed good MetH inhibition activity.
- Compound **6c** arrested tumor cell in G_1 phase and induced cell apoptosis.

The authors declare that they have no competing interests.